Prog. Energy Combust. Sci. 1993, Vol. 19, pp. 145–185
Printed in Great Britain.

0360–1285/93 $24.00

TOXIC METAL EMISSIONS FROM INCINERATION: MECHANISMS AND CONTROL

WILLIAM P. LINAK* and JOST O. L. WENDT†

* *Combustion Research Branch, MD-65, Air and Energy Engineering Research Laboratory, U.S. Environmental Protection Agency, Research Triangle Park, NC 27711, U.S.A.*

† *Department of Chemical Engineering, University of Arizona, Tucson, AZ 85721, U.S.A*

Received 8 April 1993

Abstract—Toxic metals appear in the effluents of many combustion processes, and their release into the environment has come under regulatory scrutiny. This paper reviews the nature of the problems associated with toxic metals in combustion processes, and describes where these problems occur and how they are addressed through current and proposed regulations. Although emphasis in this paper is on problems associated with metals from incineration processes, conventional fossil fuel combustion is also considered, insofar as it pertains to mechanisms governing the fate of metals during combustion in general. This paper examines the release of metals into the vapor phase, with the particle dynamics of a nucleating, condensing, and coagulating aerosol that may be subsequently formed, and with the reactive scavenging of metals by sorbents.

Metals can be introduced into combustion chambers in many physical and chemical forms. The subsequent transformations and vaporization of any volatile metal depend on the combustion environment, the presence of chlorine and other species (reducing or oxidizing), on the nature of the reactive metallic species formed within the furnace, and on the presence of other inorganic species such as alumino-silicates. Some insight into how these factors influence metal release can be gained by considering the release of organic sodium during coal char combustion.

Once vaporized, a metal vapor cloud will normally pass through its dewpoint to form tiny nuclei, or condense around existing particles. These aerosols are then affected by other dynamic processes (including coagulation) as they evolve with time. This paper shows how current mathematical descriptions of aerosol dynamics are very useful in predicting metal aerosol size distributions in combustion systems. These models are applied to two prototype problems, namely: the prediction of the temporal evolution of a particle size distribution of a self-coagulating aerosol initially composed of nuclei; and the scavenging of nuclei by coagulation with larger sorbent particles.

A metal vapor can also react with certain aluminosilicate sorbents. This process, which will occur at temperatures above the dewpoint, is described, and is important, since it allows the high temperatures in incineration processes to be exploited to allow the formation of water-unleachable metal-containing compounds that can be isolated from the environment. Future research problems are also identified.

CONTENTS

* Corresponding author.

1. INTRODUCTION

A major impediment to public acceptance of incineration as a disposal option for hazardous and/or municipal wastes, is the release of toxic metals into the environment.[1–4] Many hazardous and municipal waste streams contain metal constituents, which, upon being subjected to combustion environments, may be transformed into species and physical forms that are substantially different from those which entered. As a result, these conditions greatly affect how metal constituents are released into the environment. This paper reviews and evaluates the current understanding of mechanisms governing the fate of metal during combustion. Emphasis is on processes occurring in hazardous and municipal waste incinerators, rather than in fossil fuel combustors, although the copious literature on the latter is not disregarded insofar as it yields information on metal transformation mechanisms in a generic sense.

We arbitrarily restrict our scope to mechanisms governing metal transformations in a combustor. The behavior of flue gas particulate collection devices, *per se*, is outside the scope of this review, although the manner in which combustion conditions themselves can influence the collection and isolation of metals from the environment, is not. Section 2 identifies toxic metals of concern and how regulations are being developed to address their control. Section 3 presents background information which identifies the problem's scope and multimedia considerations, and then reviews existing literature on the occurrence of toxic metals in combustion systems including pulverized coal, fuel oil, hazardous wastes, municipal wastes, industrial processes, and sewage sludge. Section 4 presents a mechanistic overview of metal behavior in combustion systems. Section 5 discusses theoretical and experimental efforts which have examined how metals partition with respect to both particle size and chemical species in combustion systems. Further detailed discussion of fundamental aerosol dynamics is presented in Section 6, which then goes on to show how empirical data and theory can be used together to identify controlling mechanisms that describe aerosol evolution. Section 7 presents the results of several studies that are proposing the use of sorbents to capture metal in combustion environments including flowing ducts, fixed beds, and fluidized beds. Finally, Section 8 presents some conclusions and identifies future research problems.

Mechanisms governing the potential *control* of airborne metal emissions through sorbent injection into the combustor will be covered (Section 7), since this is directly related to metal transformations and aerosol dynamics in the combustion chamber. Furthermore, we shall discuss mechanisms in a generic sense, applicable to a range of incineration and combustion equipment, rather than focusing on the hardware details of a specific type of incinerator. However, the relationship between fundamental mechanisms and relevant practical problems related to the presence of metals in a combustion system, is a central feature of this work. We hope, thereby, to assist both the practising engineer, whose objectives range from specifying incinerator designs to devising test-burn protocols and permit applications, and the combustion researcher, who wishes to address scientifically interesting and challenging relevant problems.

2. IDENTIFICATION AND REGULATION OF TOXIC METALS

2.1. *Health Effects*

Toxic metals are identified by their adverse effects on human health. Numerous studies have examined metal toxicity (e.g. mutagenicity, carcinogenicity, and damage to different organs or systems such as the liver, kidneys, and the hemopoietic, reproductive, nervous, and immune systems), and it is certainly outside the scope of this review to address this topic in any detail. However, adverse health effects are the primary reason that metal emissions are regulated, and for this reason discussion of the subject is important. Goyer[5] in a review of the toxic effects of metals points out that of the approximately 80 elements that exhibit metallic or metal-like properties approximately 30 form compounds that have been reported to produce toxicity in humans. This review grouped toxic metals into four categories: major toxic metals

with multiple effects (arsenic, beryllium, cadmium, chromium, lead, mercury, and nickel); essential metals with potential for toxicity (cobalt, copper, iron, manganese, molybdenum, selenium, and zinc); metals with toxicity related to medical therapy (aluminum, bismuth, gallium, gold, lithium, and platinum); and minor toxic metals (antimony, barium, indium, magnesium, silver, tellurium, thallium, tin, titanium, uranium, and vanadium).

Metals have both geological and biological cycles within the environment. The geological cycle includes rainwater dissolution of metals in rocks, ores, and soils, and transportation via surface waters to lakes and oceans to precipitate as sediment or be taken up by rainwater to be redeposited elsewhere. The biological cycle includes bioaccumulation in plants and animals and movement throughout the food chain.[5] The amount of metals from natural sources moving through these cycles may be greater than any anthropogenic contribution; however, human industrial activity may greatly enhance metal release rates from ores, emit new compounds not naturally occurring in the environment, and greatly increase worldwide distribution.[5] For humans in general, food sources and ingestion likely represent the largest metals exposure route, with additional contribution from the air. Other potential routes for exposure include consumer products, industrial wastes, and the working environment.[5]

Vouk and Piver[6] in their review of the carcinogenicity and mutagenicity of metallic emissions from fossil fuel combustion, identified a group of metals including arsenic, beryllium, cadmium, chromium, nickel, and possibly antimony and selenium as potential human carcinogens contained in air pollutants derived from fossil fuel combustion. This subset does not include the naturally radioactive carcinogenic elements (thorium and uranium) or elements for which animal carcinomas could be induced only under special circumstances or through exposure by specific metal compounds (aluminum, cobalt, copper, gadolinium, iron, lead, manganese, mercury, platinum, titanium, silver, ytterbium, and zinc). Conversely, Vouk and Piver[6] report on studies that show negative carcinogenic results for germanium, tellurium, tin, and vanadium. Caution is necessary, however, because most of these data are the result of animal studies that may or may not be representative of similar effects in humans. Also, lack of carcinogenicity does not mean that a metal cannot cause other adverse effects. The limited human case reports or epidemiological data that are available (typically through occupational exposure) tend to corroborate the animal studies showing that the specific compounds of arsenic, beryllium, cadmium, chromium, and nickel, and the compounds of the naturally radioactive elements thorium and uranium contribute to human cancer.[6]

Metallic elements do not biodegrade and, once absorbed or ingested, they tend to bioaccumulate until excreted. Mercury has a particularly high ability to bioaccumulate.[7] Because of its high vapor pressure, mercury is emitted from combustion systems primarily as a vapor. Mercury has a long atmospheric half life and is deposited most commonly as the divalent ion where it is methylated by microorganisms to methylmercury.[7] Bioaccumulation in fish with subsequent fish consumption is the primary human exposure route. Methylmercury is mobile in the body and readily crosses the human placenta.[8] Mercury irreparably damages the central nervous system causing a host of neurological problems, including birth defects and developmental impairment in children.[8]

Lead also causes permanent and untreatable damage to the central and peripheral nervous systems; in addition, lead is associated with renal damage, hypertension, and reproductive and birth defects.[9] Landrigan[9] describes lead as a subclinical toxin, which denotes a class of chemicals that may cause harmful effects at low dose exposure that are not readily evident with a standard clinical examination. Sarofim and Suk[10] describe the work of Needleman, who has shown IQ reductions (7 to 8 points) in children exposed to low and high lead levels. Further mental development scores showed a clear gap between groups of children whose average blood levels at birth were 1.8 and 14 $\mu g\ l^{-1}$. Sarofim and Suk[10] report that the Center for Disease Control's lead cautionary blood level is 25 $\mu g\ l^{-1}$.

It should be noted that the complex field of toxic metal epidemiology is incomplete and contains many uncertainties, and so, a definitive review of that subject is outside the scope of this paper. However, in summary, it may be concluded that toxic metals can affect human health in numerous ways that are both obvious and subtle. This presents a difficult challenge to the environmental regulator who must identify and assess the relative additional risks caused by anthropogenic toxic metals in the environment and then devise regulations to manage the incremental health and environmental risks within acceptable levels.

2.2. *Regulations*

In the U.S., the environmental regulation addressing air emissions of toxic metals depends on whether hazardous waste incineration (HWI), municipal waste combustion/incineration (MWI), or some other (combustion) process is involved. The identification and definition of 'toxic metals' as discussed here includes classes of mutagenic, carcinogenic, and otherwise toxic metal species and depends on the nature of the regulation applied. This paper follows guidelines being developed under both the Resource Conservation and Recovery Act (RCRA, amended 1986),[11] and the Clean Air Act (CAA, amended 1990)[12] and includes under the heading toxic metals those listed in Table 1.

TABLE 1. Metals regulated under RCRA and CAA

Metal	Symbol	RCRA regulated*	CAA regulated†
Antimony	Sb	yes	yes
Arsenic	As	yes	yes
Barium	Ba	yes	no
Beryllium	Be	yes	yes
Cadmium	Cd	yes	yes
Chromium	Cr	yes	yes
Cobalt	Co	no	yes
Lead	Pb	yes	yes
Manganese	Mn	no	yes
Mercury	Hg	yes	yes
Nickel	Ni	yes	yes
Selenium	Se	yes	yes
Silver	Ag	yes	no
Thallium	Tl	yes	no

*Appendix VIII regulated as metal and compounds, not otherwise specified. Other specific metal compounds including cyanide compounds of calcium, copper, potassium, sodium, and zinc as well as oxides of vanadium (V) and osmium (VIII) are also regulated.[11] RCRA air emission limits are proposed.

†Proposed.[12]

TABLE 2. Proposed RCRA MEI concentrations corresponding to maximum allowable risk limits*

Carcinogenic metal	Risk specific dose RSD† $\mu g\ m^{-3}$
As	0.0023
Be	0.0041
Cd	0.0055
Cr‡	0.00083

Non-carcinogenic metal	Reference air conc. RAC $\mu g\ m^{-3}$
Sb	0.3
Ba	50.0
Pb	0.09
Hg	0.08
Ni	20.0
Se	4.0
Ag	3.0
Tl	0.3

*The current particulate standard is 180 mg dsm^{-3}, dsm^3 defined as dry, corrected to 293 K, 760 mm Hg, 7% oxygen.[13]

†Annual average ground level concentration resulting in 1 unit risk for MEI (70 year exposure). Note that the *sum* of carcinogenic metals risk may not exceed 1 unit risk.

‡RSD refers to Cr^{6+} compounds only. Cr^{3+} compounds are not included. However, all chromium is considered Cr^{6+} unless site specific speciation is performed.

Hazardous waste incinerators and boilers and industrial furnaces (BIFs) that destroy hazardous waste in the U.S. are regulated under RCRA. Those portions of the amended regulations addressing toxic metal emissions are based on risk assessment arguments which limit ground level concentrations that may be inhaled by the maximum exposed individual (MEI). Indirect exposure mechanisms (e.g. ingestion, dermal contact) are not considered. Additionally, exposure is assumed to result only through exposure to incinerator air emissions. The original Federal Register rule discriminates between four carcinogenic and six non-carcinogenic metals.[13] However, since the release of this notice, nickel and selenium have been included in the list of non-carcinogenic metals, and the risk data for mercury have been revised.[14]

Carcinogenic metal emissions, when summed, may not exceed an incremental lifetime risk (70 years) to the MEI greater than 1.0×10^{-5}. Ground level concentrations representing Risk Specific Doses (RSDs) for four carcinogenic metals at the 10^{-5} risk level (unit risk) are reported in Table 2. Eight non-carcinogenic metals have their ground level concentrations limited by Reference Air Concentrations (RACs, also shown in Table 2). With the exception of lead, these RACs are established as 25% of the oral-based Reference Dose (RfD), converted 1 to 1 to an inhalation RfD. The RAC for lead is established as 10% of the National Ambient Air Quality Standard (NAAQS). The incinerator (or BIF) operator may relate permissible ground level concentrations to permissible metal feed rates to the incinerator by one of three methods. The Tier I method defines allowable metal feed rates to the incinerator using a conservative 'reasonable worst case' stack dispersion model and does not account for any metal partitioning or particulate removal within the incinerator or its air pollution control system (APCS). This method assumes 100% emission of any metal feed with the stack gases. The Tier II method includes the same Tier I dispersion calculation but does account for metal partitioning and APCS removal efficiencies obtained by site specific emission testing. As a result, the Tier II method defines allowable stack emission rates of toxic metals (after the APCS). These Tier II stack emission limits correspond to the Tier I feed limits. The Tier III method also involves emission testing and requires site specific dispersion modeling. Typically, the Tier I approach is the simplest to implement but also results in the lowest allowable metal feed rates. Conversely, the Tier III approach is the most lenient with respect to allowable metal feed rates, but imposes the most rigorous burden on the incinerator owner/operator to characterize the behavior of toxic metals within and around the facility.

The risk approach by which metal emissions are regulated by RCRA is significantly different than many technology based regulations often mandated by other legislation. As a result, it is difficult to directly compare relative emission limits between RCRA devices and other combustion or incineration systems regulated in the U.S. and other countries. However, such a comparison is useful and is possible if a specific incinerator is examined or assumptions are made regarding a hypothetical incinerator. Consider an 8.8 MW (30×10^6 Btu hr^{-1}) rotary kiln

TABLE 3. Proposed RCRA metal emission limits for a hypothetical 8.8 MW rotary kiln incinerator corresponding to a Tier II analysis*

	Emission rate g hr^{-1}	Concentration‡ mg Nm^{-3}	Concentration§ dry, 11% O_2 mg Nm^{-3}
Carcinogenic metal†			
As	0.82	0.051	0.056
Be	1.5	0.093	0.103
Cd	2.0	0.12	0.14
Cr‖	0.30	0.019	0.021
Non-carcinogenic metal			
Sb	110	6.8	7.5
Ba	18000	1110	1230
Pb	32	2.0	3.6
Hg	29	1.8	2.2
Ni	7300	450	500
Se	1500	93	103
Ag	1100	68	75
Tl	110	6.8	7.5

*Based on 8.8 MW, 16,200 Nm^3 hr^{-1} flow rate (100% excess air), rural location, non-complex terrain, no impinging structures, 15.25 m stack height, 355 K stack gas temperature.[13]

†Carcinogenic metal emissions resulting in 1 unit risk. Note that the *sum* of carcinogenic metals risk may not exceed 1 unit risk.

‡Emission rate divided by volumetric flow (wet), not corrected to dry, standard oxygen conditions. Calculated stack gas contains 10% water and 11% oxygen.

§Corrected to dry, 11% oxygen conditions (EC convention).

‖RSD refers to Cr^{6+} compounds only. Cr^{3+} compounds are not included. However, all chromium is considered Cr^{6+} unless site specific speciation is performed.

incinerator located in a rural area with non-complex (flat) terrain and no large buildings or structures nearby to complicate the plume behavior. The value 8.8 MW represents an average for rotary kiln incinerators in operation in the U.S.[15] If we further assume that this hypothetical rotary kiln operates with 100% excess air (stoichiometric ratio = 2.0), then an approximate system volumetric flow rate of 16,200 Nm^3 hr^{-1} can be calculated. Other necessary assumptions include stack height (15.25 m) and stack gas exit temperature (355 K). Using these parameters, a Tier II analysis[13] would allow maximum metal emission rates (and corresponding metal stack concentrations) as presented in Table 3. These emission rates are taken directly from look-up tables in the Federal Register notice,[13] but can also be calculated directly knowing the allowable RACs or RSDs and a dispersion coefficient determined from the 'reasonable worst case' or site specific models by:

$$\text{Allowable emission rate} = \frac{\text{Allowable RAC or RSD}}{\text{Dispersion coefficient}}. \quad (1)$$

For the scenario presented here, the Tier II dispersion model calculates a dispersion coefficient of 2.75×10^{-3} (μg m^{-3})/(g hr^{-1}). Note that the emissions for the carcinogenic metals (Table 3) are based on individual unit risk calculations; however, actual emissions must be such that the *sum* of these emissions must be less than 1 unit risk. If multiple carcinogenic metals are involved, the individual emissions must be evaluated according to:

$$\sum_{i=1}^{n} \frac{\text{Actual emission}_i}{\text{Tier II emission limit}_i} \leq 1. \quad (2)$$

Evident from Table 3 is that the risk limits cause the carcinogenic metals to be controlled to a much lower level than the non-carcinogenic metals. In fact, in this scenario, the barium limit (1110 mg Nm^{-3}) is over six times the allowable total particulate limit (180 mg Nm^{-3}).[13] This example provides an analysis based on a hypothetical situation. Emission limits for other situations may be quite different. However, due to the conservatism built into the Tier II screening limits, emission limits under Tier III can be a factor of 10 or more higher than those under Tier II.[13]

Title III of the CAA places limits on the emissions of 189 organic and metallic hazardous air pollutants (HAPs), including emissions from a variety of combustion sources such as industrial furnaces and boilers. Furthermore, studies are underway to assess the health risk associated with HAP compounds from utility boilers to determine whether these sources should also be regulated. With the CAA currently calling for control of combined listed HAP emissions greater than 22,727 kg $year^{-1}$ (25 tons $year^{-1}$) or 9,091 kg $year^{-1}$ (10 tons $year^{-1}$) of a single listed compound from any regulated source, exceedingly low concentrations in large flue gas streams may result in noncompliance. For example, using the average EPA lead emission factor for an uncontrolled dry-bottom bituminous pulverized-coal utility boiler of 4.89×10^{-7} kg kW-hr^{-1} (316 lb/10^{12} Btu),[16] a 500

TABLE 4. Proposed CAA metal regulations for municipal waste incinerators

Metal	$< 225 \times 10^6$ g day^{-1} (< 9.4 tonnes hr^{-1}) mg Nm^{-3}*	$225–1000 \times 10^6$ g day^{-1} (9.4–41.7 tonnes hr^{-1}) mg Nm^{-3}	$> 1000 \times 10^6$ g day^{-1} (> 41.7 tonnes hr^{-1}) mg Nm^{-3}
Particulate	†	existing—69/new‡—34	34
Cd	†	§	§
Pb	†	§	§
Hg	†	§	§

*Defined as dry, corrected to 273 K, 760 mm Hg, 7% oxygen.[19] 1×10^6 g = 1 tonne (metric) = 1.1 tons (English).

†Particulate and Cd, Pb, and Hg emission limits for these units are anticipated as per Section 129 of CAA, but not yet quantified.[12]

‡New units defined as those that commenced construction after December 20, 1989.

§Cd, Pb, and Hg emission limits for these units anticipated as per Section 129 of CAA, but not yet quantified.[12]

TABLE 5. Proposed EC metal regulations for hazardous and municipal waste incinerators

Hazardous waste incinerators

Metal	Concentration mg Nm^{-3}*
Particulate	5† or 10‡
ΣCd + Tl	0.05
Hg	0.05
ΣSb + As + Co + Cu + Cr + Pb + Mn + Ni + Sn + V	0.5

Municipal waste incinerators

Metal	< 1 tonnes hr^{-1} mg Nm^{-3}§	1–3 tonnes hr^{-1} mg Nm^{-3}	> 3 tonnes hr^{-1} mg Nm^{-3}
Particulate	200	100	30
ΣCd + Hg	—	0.2	0.2
ΣAs + Ni	—	1.0	1.0
ΣCu + Cr + Pb + Mn	—	5.0	5.0

*Defined as dry, corrected to 273 K, 101.3 kPa, 11% oxygen (1992 EC Directive, from Millot[21]).

†Daily average.

‡Half-hour average.

§Defined as dry, corrected to 273 K, 101.3 kPa, 9% carbon dioxide (1989 EC Directive, from Scott[20]).

MWe unit operating with a 34% thermal efficiency and an 80% capacity factor emits approximately 5,455 kg year^{-1} (6 tons year^{-1}) of lead (as PbO). An electrostatic precipitator (ESP) may reduce this emission by approximately a factor of six (909 kg year^{-1}, 1 ton year^{-1}).[16] Note that this calculation uses an average emission factor. Lead concentrations in American coals have been shown to vary by over a factor of 60.[17,18] Large concentration variations are also common within coal mined at different times from the same location. Also considering that the emissions from the sources will probably include multiple HAP compounds, both organic and inorganic, each present in concentrations varying over several orders of magnitude, the complexity of the problem becomes evident. Also note, however, that specific regulations controlling metal emissions under the CAA have not been promulgated, and as far as HWI regulations are concerned, CAA requirements are to be consistent with RCRA. MWI metal emissions will also be limited under Title III of the CAA. The proposed metal regulatory limits for these special units are shown in Table 4.[19]

To form a basis for comparison, Table 5 presents metal emission regulations proposed or in effect for the European Community (EC) for both hazardous and municipal waste incinerators.[20,21] The intent of the EC directives are to establish minimum emission standards for all EC members. As is the case for individual U.S. states, each EC member state may require emission limits more stringent than the EC directive. Germany, for example, had proposed similar metal limits in 1990 when the EC directive limits for HWIs were approximately two times higher.[22,23] Millot[21] presents the results of a French trial burn at a new EMC Services Salaise Sur Sanne HWI. This incinerator equipped with an ESP, wet lime injection, dynamic venturi, wet soda injection, and electro-

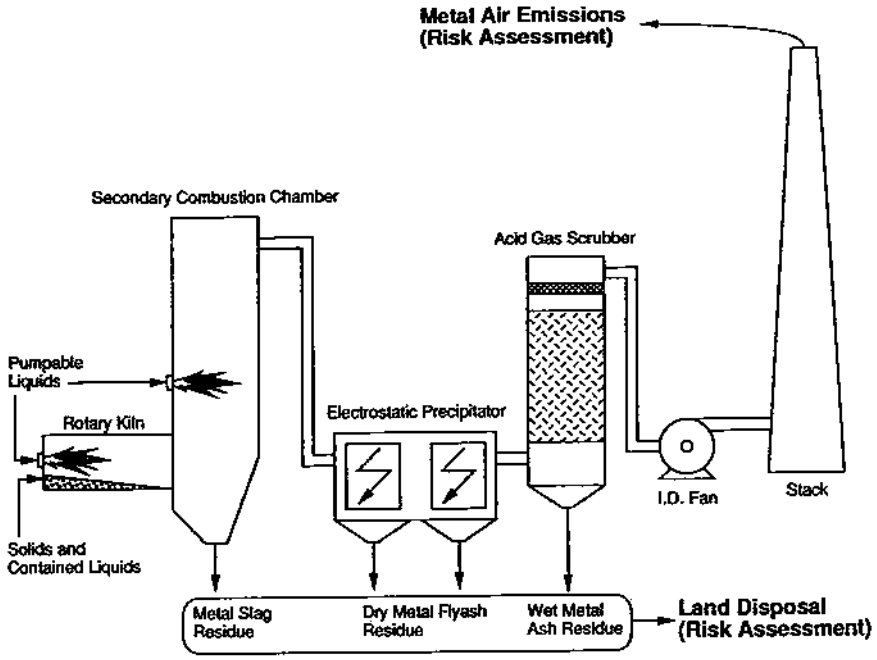

FIG. 1. Metal multimedia considerations at incineration facilities.

dynamic venturi demonstrated that these EC metal limits are achievable. The EMC tests found ΣCd + Tl = 0.001–0.005 mg Nm^{-3}, Hg = 0.005–0.010 mg Nm^{-3}, and Σ other regulated metals (see Table 5) = 0.05–0.08 mg Nm^{-3}. Unlike the proposed U.S. regulations, the proposed EC regulations include limits on cobalt, copper, manganese, tin, and vanadium for HWIs, and arsenic, chromium, copper, manganese, and nickel for MWIs. While copper exhibits some toxic characteristics, it is probably included because of its suspected catalytic enhancement of polychlorinated dibenzodioxin (PCDD) and polychlorinated dibenzofuran (PCDF) formation mechanisms.[24–32] Conversely, the proposed U.S. regulations include limits on beryllium, barium, selenium, and silver for HWIs, while the EC limits do not include these metals. Comparison of the proposed risk-based RCRA emissions limits (Tier II) calculated in Table 3 for a hypothetical incinerator with the proposed EC emission limits in Table 5 shows, in general, comparable emission limits placed on four RCRA carcinogenic metals, and less stringent limits on the RCRA non-carcinogenic metals compared to the EC directives.

3. BACKGROUND

3.1. *Multimedia Considerations*

The preceding section addressed regulations on emissions of toxic metals into the air environment. Additionally important, however, is the release of metals into the water and land environments. Therefore, it is appropriate to address the multimedia aspects of toxic metal behavior in incineration processes.

Figure 1 depicts a typical HWI facility, used as a practical example to demonstrate the importance of considering multimedia, rather than merely air pollution, concerns. Similar arguments can be made for MWIs and other combustion sources. In this HWI, wastes containing metal components are introduced into a rotary kiln or injected as liquids into the secondary combustion chamber (SCC), at the left-hand side of the figure. In the kiln, some fraction of the toxic metals may form a slag with other inorganic components forming for example silicon, aluminum, calcium, and iron complex mixtures which can be removed as a solid at the kiln exit. Incorporation of toxic metals into the solid slag can be quite desirable, and the science behind the application of slag technology to recycling or disposal of solid wastes has been discussed by Queneau *et al.*[33] and Smith.[34] Ideally, any unrecovered toxic metal in the slag will not be water leachable, in order for that waste residue to be delisted for subsequent disposal in a nonisolated landfill.

A significant portion of the toxic metals, however, may become entrained in the gas phase or vaporized to form a gas or airborne aerosol in the combustion chambers or farther downstream. Possible mechanisms for this are discussed in later sections. This airborne material may be swept through the SCC, where additional metal transformations may take place, and may be subsequently removed by multiple particulate control devices. In Fig. 1, an ESP removes much of the material in question. The removal efficiency depends on the type of device, particle size,

and possibly species where small particles (0.1–1.0 μm in diameter) are typically most difficult to remove. From the ESP, a dry metal flyash residue is collected and must be disposed of properly. As with the kiln slag, the toxicity and leachability of this flyash residue will determine the ease with which it must subsequently be handled, and these properties are governed in part by what happens in the two combustion chambers (kiln and SCC). Note that this residue is likely to have significantly different chemical and physical characteristics from those of the slag and kiln bottom ash that has been removed upstream.

Downstream of the ESP, Fig. 1 shows a caustic wet scrubber whose purpose is to remove (and neutralize) acid gases (e.g. HCl, SO_2). This device may also remove some particles that had escaped the ESP. Here, the captured metal enters the environment dissolved or suspended as an aqueous waste or as a wet metal residue, and precautions similar to those outlined above for the slag and flyash are applicable before this waste can be disposed of. Finally, some fraction of the metal constituents will escape all particulate and acid gas control devices and exit through the stack. These are the emissions that are controlled through Tier II and Tier III regulations under RCRA (Tier I assumes that all the metal in question exits the stack). As mentioned previously, RCRA assumes that inhalation is the primary mechanism through which humans are exposed to risk. This methodology, however, may underpredict exposure. Once emitted, metals may directly impact human health through inhalation, and also through indirect (non-inhalation) exposure pathways including incidental soil ingestion, plant ingestion, dermal absorption, mother's milk, fish, dairy, meat, and water. Assessing the relative contribution among these pathways is extremely difficult with many assumptions and uncertainties. Methods to apportion this exposure are being developed,[35,36] and reveal that the magnitude of exposure from indirect (non-inhalation) pathways ranges widely depending on the scenario examined. However, these calculations predict that the indirect contribution may be significant, ranging from a small fraction (several %) to a major fraction (over 90%) of the total.[37]

As shown in Fig. 1, the fate of toxic metals is a multimedia problem with potential impacts on all three environments, land, water, and air. It is shown below that the combustion process can determine the extent to which any particular combination of toxic metals impacts these media. Unlike organic constituents, metals are not destroyed by incineration. However, incineration environments may cause metals to be transformed (physically and chemically) and transferred from one medium to another. One mission of researchers in this area could be to devise methods that, through modification of the combustion process and improvements in air pollution control technology, minimize the *multimedia* impact, not merely the air impact, of toxic metals.

3.2. *Occurrence of Toxic Metals in Combustion Systems*

While the previous section was concerned with the chemical and physical forms in which toxic metals leave an incineration process, it is appropriate now to consider how these metals are introduced to these processes. The occurrence of toxic trace elements associated with airborne particulate matter has been reviewed by Schroeder *et al.*[38] They arise from the combustion of coal, oil, hazardous wastes, municipal wastes, and sewage sludge. Industrial processes, such as cement kilns, are also contributors. Each of these potential sources is now discussed in turn.

3.2.1. *Pulverized coal*

The formation of ash, and the transformation of mineral matter during coal combustion, have been topics of intensive study by numerous research groups. Industrial research laboratories (coal suppliers and boiler manufacturers) have long been involved with ash deposition (fouling and slagging) studies, and these have been well covered in the treatise by Raask.[39] Several recent studies[40–45] were directed towards predicting the composition of the size-segregated ash aerosol evolving throughout the combustor and towards characterizing and controlling the corrosion, fouling, slagging, and other detrimental effects these species have on combustor materials and heat transfer surfaces.[39] The metal particle formation and evolution mechanisms identified by these studies are directly applicable to environmental research.

Metals have been identifed to exist in pulverized coal in three ways. *Included* mineral matter exists as inorganic entities trapped as crystalline or glassy structures throughout fuel particles containing appreciable carbon and hydrogen. *Inherent* mineral matter is chemically bound as individual atoms within the coal organic matrix. *Excluded* mineral matter consists of particles distinct and separate from those containing primarily combustible fuels, either released through the grinding process (once having been included) or originating from overburden added through the mining/ transportation process. Gluskoter[46] has reported on this ash breakdown for various coals, and Linak and Peterson[47] indicate that inherent ash content is an important factor in determining a coal's propensity to produce submicron ash particles. The fact that toxic and heavy metal constituents are associated with pulverized coal ash has been known for many years. Table 6 presents concentration ranges of inorganic species found in American coals taken from Hardesty and Pohl.[18] Their data show that there is a considerable

TABLE 6. Concentration ranges of inorganic elements found in American coals (adapted from Hardesty and Pohl[18])*

Element	Concentration range ppm†
Si	5000–410000
Al	3000–23000
Fe	340–23000
Ca	50–12300
S	300–10000
K	100–6500
Na	100–6000
Mg	240–3500
Ti	200–1800
Ba	20–1600
Sr	17–1000
Cr	100–400
Zr	28–300
P	6–300
Sn	1–400
Cl	10–260
Mn	5–240
Cu	3–250
B	1–230
Rb	1–150
F	1–110
Co	1–90
Zn	3–80
V	2–77
Ni	2–60
Li	4–63
Nb	5–41
As	1–60
Pb	1–60
Ga	0.3–60
Nd	4–30
Sc	3–30
Ce	1–30
Y	3–25
Br	1–23
La	0.3–29
Sb	0.1–30

* Other elements < 10 ppm by weight.
† By weight.

range of values for each element, among the coals considered. In addition, Holcombe *et al.*[48] have shown that, even for a single power plant, there is considerable variation between samples. The copious literature on trace metals in coal ash has been reviewed previously by Nettleton[49] and Smith.[50] Mechanisms of ash particle formation from pulverized coal combustion have been suggested by Flagan and Friedlander[17] and experimentally investigated by Okazaki *et al.*,[51] Sarofim and co-workers at MIT, and Flagan and co-workers at Cal Tech. Data on the size segregated emission of toxic metals from field combustion units have been released by Davison *et al.*,[52] Kaakinen *et al.*,[53] Klein *et al.*,[54] White *et al.*,[55] Markowski and Filby,[56] and Kauppinen and Pakkanen,[57] to name but a few. Andren *et al.*[58] focused on selenium and Billings and Matson[59] examined mercury. All these data show that submicron particles are greatly enriched in many of the toxic metals discussed in Section 2. Furthermore, it will be shown in a later section, that a metal's propensity to become enriched in the submicron aerosol fraction is related, in part, to its vapor pressure at combustion temperatures.

Table 7 summarizes coal combustion data taken from the literature from a wide range of laboratory and full scale sources which have examined enrichment trends of toxic and other metal and inorganic species with respect to particle size.[47,52–54,57,60–76] While there is some variation in enrichment trends among the authors for specific species, the data, in general, consistently show enrichment of most toxic metals of interest in the submicron flyash fraction. This submicron enrichment trend is clearly evident for the metals, antimony, arsenic, cadmium, chromium, lead, mercury, nickel, and selenium. The submicron enrichment trends for barium, beryllium, cobalt, and manganese are less conclusive. Finally, the metals, silver and thallium, were not examined in sufficient detail to draw conclusions. These enrichment trends, however, are not absolute, Davison *et al.*,[52] for example, show that lead is also found in significant concentrations on larger particles, those greater than 10 μm in diameter. Therefore, the issue is to explain not only the elemental enrichment in small particles, which, as shown below, follows from vaporization and nucleation/condensation of certain toxic metals, but also the presence of the same (presumably volatile) metals in the larger particles. In other words, although the data generally show that volatile elements tend to concentrate on submicron particles, this is not universally the case, and there are examples of volatile elements being captured (or retained) within larger flyash particles. It remains to be seen what factors in coal composition and combustion conditions can account for high fractions of volatile metal appearing in the submicron size range in one case but not the other.

That submicron particles, which may be greatly enriched in toxic metals, are less efficiently collected than supermicron particles has been shown by McCain *et al.*[77] and Ondov *et al.*,[63] for ESPs. McCain *et al.*[77] examined five full scale ESPs and found moderately high to high particulate collection efficiencies (98–99.9%) for particles with diameters larger than a few microns or smaller than a few hundredths of a micron and a minimum collection efficiency (80–96%) for particles having diameters of a few tenths of a micron. Ondov *et al.*[63] show that even a cold-side ESP, designed for an overall collection efficiency of 99.7% by weight, was only partially successful in removing the submicron flyash particles. Seeker[78,79] presents typical particle size dependent removal efficiency curves for venturi scrubbers, high efficiency particulate air (HEPA) filters, and ESPs. All three devices exhibited minimum collection efficiences for a range of submicron particle diameters. This size dependent collection efficiency is further illustrated in Fig. 2 by Markowski *et al.*,[68] and shows that, although the submicron fraction before particulate control may contain less

TABLE 7. Coal combustion investigations describing submicron flyash elemental enrichment (adapted from Linak and Peterson[47])

Investigation	Submicron enriched	No enrichment trend	Submicron depleted
Biermann and Ondov[67]	Ba, Se, U, W	Fe, Na	
Coles *et al.*[61]	Pb, Ra, Th, U	Ce	
Damle *et al.*[70]*	Sb, As, Cd, Pb, Mo, Se, W, Zn	†Ba, Cr, Co, Ni, Mn, Na, Sr, V	‡Al, Ca, Ce, Hf, Fe, Mg, K, Si, Ti
Davison *et al.*[52]	Sb, As, Cd, Cr, Pb, Ni, Se, S, Tl, Zn	Al, Be, C, Fe, Mg, Mn, Si, V	Bi, Ca, Co, Cu, K, Sn, Ti
Desrosiers *et al.*[64]	Si, S	Ca, Mg, K, Na	Al, Fe
Flagan and Taylor[69]	C, Si, Na, S		
Gladney *et al.*[60]	Sb, As, Br, I, Pb, Hg, Se	Na	Ce, Fe
Haynes *et al.*[72]	Sb, As, Fe, Mn, Hg, K	Mg	Al, Ca, Si
Kaakinen *et al.*[53]	Sb, As, Cu, Pb, Mo, Po, Se, Zn	Al, Fe, Nb, Rb, Sr, Y	
Kauppinen and Pakkanen[57]	Ca, Cd, Cu, Pb, Sr, S, V	Al, Fe, Mg, Mn, Na, Si, Ti, Zn	
Klein *et al.*[54]§	Sb, As, Cd, Cu, Cr, Ga, Pb, Mo, Ni, Se, Na, U, V, Zn	Al, Ba, Ca, Ce, Co, Eu, Hf, Fe, La, Mg, Mn, K, Rb, Sc, Si, Sm, Sr, Ta, Th, Ti	
Linak and Peterson[47]	As, Pb, K, Na, Zn	Al, Ca, Fe, Mg, Mn, Si, Ti	
Markowski *et al.*[68]	Sb, As, Cd, Cr, Ni, Rb, Se, V, Zn	Fe, Ti	Al, Hf, Mg, Mn, Ta
Neville and Sarofim[71]	Al, Sb, As, Si, Na	Fe, Mg	
Neville *et al.*[75]	Al, Sb, As, Cr, Na, Zn	Ca, Fe, Mg	
Ondov *et al.*[62]	Sb, As, Ba, Ga, In, Mo, Se, U, V, W, Zn		
Ondov *et al.*[63]	Sb, As, Ba, Mo, Se, V, W		
Quann and Sarofim[73]	Mg, K, Na		
Quann *et al.*[74]	Sb, As, Cr, Cl, Co, Mg, P, K, Na, Zn		Al, Sc, Th
Shendrikar *et al.*[76]	Sb, As, Cl, Hg, Ni, Se, Zn		Al, Ca, Mg
Smith *et al.*[65]	Sb, As, Br, Cu, Cr, Ga, Pb, Hg, Mo, Ni, Se, S, Sn, V, Zn	Fe, Mg	
Smith *et al.*[66]‖	As, Cu, Cr, Ga, Ge, Pb, Mo, Ni, Se, Sn, V, Zn	Al, Ba, Ca, Ce, Fe, La, Mn, Nb, K, Rb, Si, Sr, Ti, Y, Zr	

* Literature review.
† Slight enrichment or no change.
‡ No change or slight depletion.
§ Species Br, Cl, Hg, Se in vapor phase, high filter penetration.
‖ Species As, Br, Cl, I, Hg, Se in vapor phase, high filter penetration.

than 5% of the total mass, the submicron mass exiting a high-efficiency ESP is comparable to that of the supermicron fraction. In fact, all particulate control devices exhibit size dependent collection efficiencies with minimum efficiencies typically seen for submicron particles in the range of 0.1–1.0 μm in diameter. These particles contain neither the mass (momentum) to be removed by impaction nor the high diffusional velocities necessary to migrate to collection surfaces. This is why, for coal combustion at least, we are concerned with the composition of the minor fraction of the total mass that might comprise the submicron particle size mode. In this context, however, new APCS devices for improved removal of submicron particles are now available (such as condensing ESPs and high efficiency bag houses),[80,81] but they are expensive and often difficult to retrofit on existing systems. Additionally, note that the metal speciation of the particles collected is still of paramount importance, since disposal must occur with minimal impact on the environment.[82,83]

As will be presented in greater detail in later sections, vaporization and subsequent heterogeneous condensation on the surface of existing particles is one mechanism by which volatile metals are transformed during combustion. Once vaporized, metal condensation is controlled by a metal species' vapor pressure relative to its equilibrium (saturation) vapor pressure. Decreasing temperatures in the post-flame regions cause supersaturation conditions that force particle formation. Heterogeneous condensation is surface-area-dependent, and particle sizes which offer the greatest surface area will accumulate the greatest proportion of the condensing metal. Linton *et al.*,[84] Smith *et al.*,[65] Neville and Sarofim,[71] Linak and Peterson,[47] and others, have shown that a number of minor and trace elements (arsenic, beryllium, calcium, carbon, chromium, lead, lithium, manganese, phosphorus, potassium, sodium, sulfur, thallium, vanadium, and zinc) present in coal flyash are preferentially concentrated on particle surfaces. These studies have further shown that this surface enrichment is size dependent. Figure 3 presents the submicron number, surface area, and volume distributions of a flyash aerosol measured at two locations in the con-

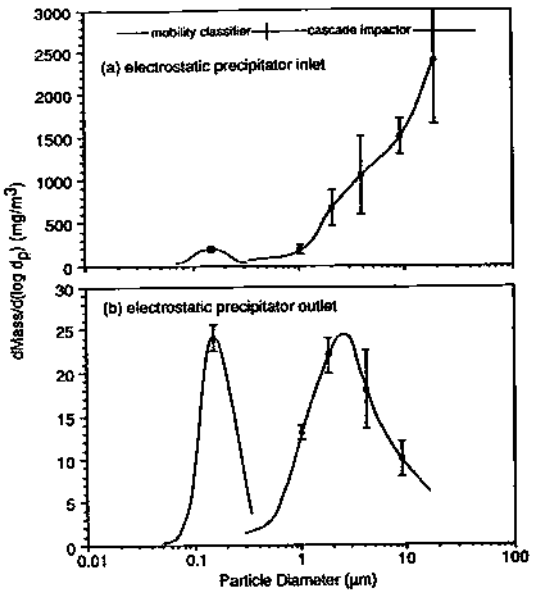

FIG. 2. Comparison of submicron and supermicron particle collection efficiency through a high efficiency electrostatic precipitator (adapted from Markowski *et al.*[68]).

vection section of a laboratory scale coal combustor burning a Utah bituminous coal.[85] Note that the volume distribution measured at the first residence time (2.7 sec) is very similar to that presented in Fig. 2a by Markowski *et al.*,[68] before particulate control. With a submicron volume concentration of approximately 4×10^{10} μm^3 m^{-3}, and a corresponding submicron mass concentration of approximately 0.1 g m^{-3}, this submicron aerosol comprises between 1 and 2% of the total ash loading. While the majority of the aerosol mass lies in the supermicron fraction, the submicron number concentration (approximately 1.3×10^{15} m^{-3}) reveals that the vast majority of the number of particles (99.9%) are submicron in size. The distribution of surface area lies somewhere in between. The surface area distribution at 2.7 sec (Fig. 3) indicates that approximately 75% of the submicron surface area resides on particles less than 0.04 μm in diameter. Submicron particles typically offer disproportionately larger surface areas compared to larger particles. Therefore, surface area dependent mechanisms such as heterogeneous condensation or surface reaction of metal vapor will likely occur preferentially around these small nuclei, promoting submicron metal enrichment.

3.2.2. *Heavy and residential fuel oil*

Typical fuel oils contain nickel and vanadium, in addition to aluminum, calcium, iron, magnesium, silicon, and sodium. Transition metals (Fe, Mn, and Co) and alkaline-earth metals (Ba, Ca, and Mg) are sometimes used for the suppression of soot.[86-89] Manganese, for example, may be added to help catalyze the combustion of residual coke cenospheres. It is important to distinguish oils from coals. In contrast to coals, oils do not contain extraneous or included mineral matter. The metals are generally inherently bound within the organic molecule, which may be the case for only a small portion of the metals (inherent) in coal. Although inherently bound, these elements are not necessarily volatile. Feldman[88] shows that non-volatile elements in heavy oils contribute to a substantial residual supermicron (> 5 μm diameter) fraction. Possible interactions between volatile metals and non-volatile minerals in oils have not been examined as they have been in coals. Oil, therefore, may not lend itself to interactions between volatile metals and non-volatile minerals, prior to the metals escaping into the bulk gas phase, unless there is a mechanism by which volatile and residual metals are drawn into proximity with one another during vaporization. Subsequent interactions between volatile and non-volatile metals, in the disperse phase, cannot be excluded, with the co-firing of other fuels or wastes or with the addition of sorbents.

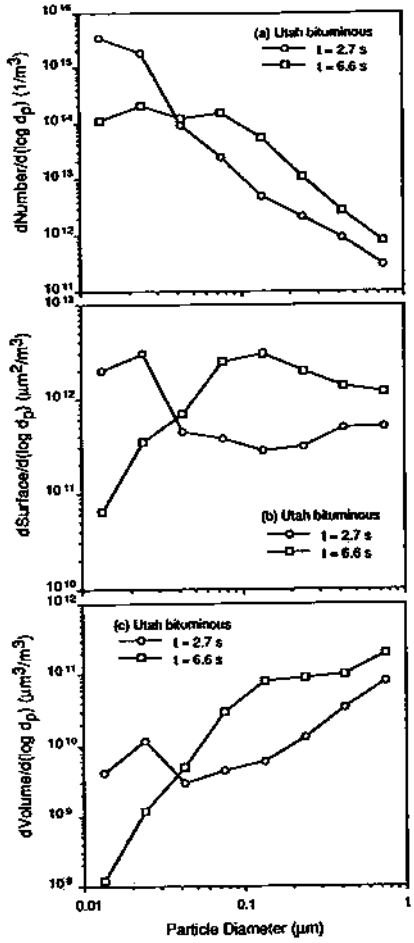

FIG. 3. Aerosol submicron (a) number, (b) surface area, and (c,) volume distributions of a coal flyash measured at two locations in the convection section of a laboratory scale coal combustor burning Utah bituminous coal (adapted from Linak and Peterson[85]).

Piper and Nazimowitz[90] and Walsh *et al.*[91] show that, in contrast to pulverized coal, the *majority* of the sampled flyash mass from residual fuel oil combustion lies below 1 μm in diameter. This is consistent with the idea that most of the initial form of the metal is inherent although the metal itself may not necessarily be volatile. Furthermore, Walsh *et al.*[91] have shown that iron, magnesium, and nickel are concentrated at the center of the submicron particles, while sodium and vanadium are associated with a 'halo of sulfate residue derived from the acid.' In fact, vanadium is a catalyst for SO_2 oxidation to SO_3. Note that, while coal-fired power plant emissions have been extensively studied, relatively limited information is available on particulate emissions from oil-fired plants. Buerki *et al.*[92] found arsenic and copper, and sometimes manganese, in the fine particle fractions from heavy fuel and residential heating oil combustion. Bacci *et al.*,[93] in an exhaustive study of particulate emissions from a large oil fired power plant, found substantial enrichment of both nickel and vanadium in the submicron particle size fraction.

3.2.3. *Hazardous wastes*

Nearly all the toxic metals listed in Table 1 can be found in hazardous wastes suitable for incineration. The ubiquitous nature of these toxic metals might be surprising. For example, lead is found in discarded batteries, soldered circuit boards, motor oil wastes, paints, dyes, and bearings. Mumford *et al.*[94] examined the toxicity of particulate emissions produced from the combustion of waste crankcase oil in small space heaters, and reported exceptionally high concentrations of lead (75.6 mg g^{-1} of collected particulate) from one atomizing oil burner. Incineration of polychlorinated biphenyl (PCB) containing capacitors often also involves the incineration of chromium, copper, lead, tin, and zinc. Chromium is contained in paints, inks, glazes, and some refractory bricks. Together with nickel, chromium is used in the manufacturing of stainless steel. Arsenic is contained in wood preservatives, insecticides, glass products, pigments, and semiconductors.[95,96] Antimony, chromium, lead, and barium are seen in high concentrations in many types of military wastes. These limited examples of metal containing (but incinerable) wastes are in addition to the more obvious by-products of modern industry, namely organometallics and aqueous metal salts, in off-specification insecticides, herbicides, and fungicides; still bottoms from refining; metallic organic and aqueous waste from the electroplating industry; and metal contaminated solvents used for machining and cleaning metal parts.

We should also consider wastes that are not normally considered to be incinerable. For example, it is often necessary to dispose of aqueous (low Btu) wastes in an incinerator, especially when these contain low concentration mixtures of metals and organic solvents not recoverable through chemical separation. In this case, the purpose of thermal treatment is to reduce the volume of the waste and, if properly performed, to yield a water unleachable solid waste to facilitate isolation of the toxic metals from the environment. Future research in chemical or biochemical separation of metals from dilute aqueous complex mixtures might lead to more efficient recovery techniques. However, even then, it might be desirable to further reduce the volume of the metal containing (chelating) solvents or metal containing organic cells by incinerating them, and subsequently capturing and vitrifying the metals.

Many Superfund sites are often best remediated by incineration or thermal treatment even when the incinerable wastes may also contain significant concentrations of metals. For example, high levels of lead and chromium are found together with PCBs at the Salem Acres site in Massachusetts. Cadmium, copper, lead and zinc are found together with acetone, benzene, toluene, and other organics at the Hanover, Virginia, Superfund site. The Abbeyville site in Louisiana contains lead and chlorine in the weight percent (wt %) range, together with 5.6 wt % semi-volatiles and up to 70 wt % hydrocarbons. These examples[97,98] indicate that incineration or thermal treatment is a viable and often preferred option for the ultimate cleanup of Superfund sites, although the ultimate fate of the metals contained in these wastes may well constitute an important technical issue to be addressed.

As discussed by Seeker,[99] wastes containing metals may be introduced into a combustion chamber in a number of ways. Liquids may be atomized to form a spray of fine droplets (typical Sauter mean diameter of 100 μm), The metal composition of each drop becomes an important parameter. A pumpable, but non-atomizable, liquid or sludge may be introduced through a lance without any attempt at atomization. Organometallic or other metal-containing liquids or sludges may also be introduced into the incinerator in drums, or bound on sorbent contained in drums.[100,101] Waxes, tars, and paints may also be introduced in cans or drums, or may be heated and atomized. Solids may be introduced shredded or whole. Military munitions are often disposed of in specially designed rotary kilns where they may explode upon entry (commonly known as 'popping incinerators'). Metals may be mixed with each other, or may be introduced into a combustion chamber together with clays or soil components.[102] Fluidized bed incinerators may also be used to dispose of metal containing wastes.[103] The fate of metals under this variety of input conditions is not clear.[99]

There is much interest in characterizing and modeling the partitioning of toxic metals into the multiple effluent streams of HWIs (see Fig. 1). This is due to the realization that metal volatility and flame chemistry play important roles in determining the ultimate fate of these metals, and that the various combina-

TABLE 8. Concentration ranges of selected metals in municipal solid waste and its bottom ash, flyash, and suspended particulates (adapted from Lisk[116])*

Metal $\mu g\ g^{-1}$	MSW†	Bottom ash	Flyash	Suspended particulate
Sb	20	na‡	139–760	610–12000
As	na	na	9.4–74	81–510
Ba	47–447	80–9000	1600–3600	40–1700
Be	< 2	na	na	na
Cd	4–22	3.8–442	< 1–477	520–2100
Cr	22–96	na	730–1900	122–1800
Cl(%)		0.2–1.0	0.12–1.12	9.92
Co	< 3–5	na	25–54	3.8–28
Pb(%)	0.01–0.15	0.04–0.80	0.06–0.54	2.5–15.5
Mn(%)	0.005–0.02	0.08–39	0.20–0.85	0.03–0.57
Hg	1–4.4	0.03–3.5	0.09–25	20–2000
Ni	9–90	110–210	38.6–960	65–440
Se	na	na	1.4–13	7.0–122
Ag	< 3–7	na	52–220	84–2000
Tl	na	na	na	150
V	na	na	110–166	6–60

* $\mu g\ g^{-1}$ unless % indicated.
† Combustible fraction.
‡ Not available.

tions of APCSs available exhibit different behavior and removal efficiencies. In recent years the studies of Wallace *et al.*,[104] Mournighan *et al.*,[105] Barton *et al.*,[106,107] Lee,[108] Fournier and Waterland,[109] Fournier *et al.*,[110,111] Carroll *et al.*,[112] and Thurnau and Fournier[113] have sought to characterize metal partitioning and emissions from pilot and full scale incinerators. Barton *et al.*[106,107] developed an analytical procedure for predicting metal partitioning between residual bottom ash, captured flyash, and emitted flyash and applied this model to a municipal waste combustor with good qualitative results. Mournighan *et al.*,[105] Fournier and Waterland,[109] Fournier *et al.*,[110,111] Carroll *et al.*,[112] and Thurnau and Fournier[113] have examined metal partitioning of various metals using the pilot scale liquid injection and rotary kiln incinerators at EPA's Incineration Research Facility (IRF) in Jefferson, Arkansas. Mournighan *et al.*[105] and Thurnau and Fournier[113] focused on synthetic and Superfund antimony and arsenic wastes, while Fournier and Waterland,[109] Fournier *et al.*,[110,111] and Carroll *et al.*[112] examined multiple metals (aqueous nitrates) bound on a clay matrix in a synthetic laboratory 'soup' and two separate APCSs. Their results indicate that most metals (> 75%) were recovered in the kiln bottom ash and that a metal's relative volatility was important in determining its partitioning into the various fractions, but that this observation was not universally true especially for lead and arsenic.

A major issue currently confronted by combustion practitioners is how to conduct and evaluate a trial burn to determine whether the Tier II or Tier III restrictions can be met. How should the metal be introduced into the incinerator for the trial burn? In what physical and/or chemical form should the metal be, and does it matter? What other wastes may or may not be introduced together with the metal, and does this matter? This review addresses these questions.

3.2.4. *Municipal wastes*

Currently, approximately 16% of the municipal waste generated in the U.S. is treated at MWI facilities.[114] This amount is expected to increase as older landfills are closed and new MWI capacity is brought online. Most U.S. MWI facilities are either mass burn units (51.5%), refuse derived fuel units (21.6%), or modular units (26.9%).[115] While we define MWI here to include both incineration (non-heat recovery) and waste to energy designs, the industry typically distinguishes between the two. According to Burton,[114] the U.S. currently has 142 operating waste to energy facilities and 34 incinerators. Another 48 new units are being planned.[115] Most of these new units are waste to energy designs.

The fact that toxic metal emissions from MWI processes is a problem should not be surprising. Lisk[116] has reviewed the environmental implications of incinerator flyash, and ash disposal. Table 8, which has been adapted from that work, shows the concentration of various metals in the combustible fraction of municipal solid waste, and the concentrations of each metal in the bottom ash, collected flyash and suspended particulates which escape into the air environment. Note the considerable enrichment of antimony, cadmium, chromium, and mercury in the suspended particulate (fine particle size range). Also important is the large amount of chlorine present since, as will be shown, this often increases metal volatilities. The suspended particulate data presented by Lisk (Table 8) represent a compilation of values gathered by measurements made by several research groups during the past 15 years. These data do not include a breakdown of the relative mass fractions of ash in the various output streams. However, examination of test data from a similar mass burn unit with a redesigned combustion chamber and equipped with a two stage ESP[117] indicates that municipal refuse typically contains between 30 and 40% water and between 15 and 35% noncombustibles and ash. Of these non-combustible materials, approximately 95% will remain to be removed from the incinerator chamber, another 2% will deposit in the boiler, and approximately 3% will be removed by the ESP. Typically much less than 1% of the ash will be emitted with the stack gases. However, even a small 10 tonne hr^{-1} unit may emit as much as 1 to 2.5 kg hr^{-1} of particulate matter.[117] Prior to its combustion chamber modifications in 1985, the particulate emissions from this unit were over 10 times higher.[117] The APCS devices associated with these measurements represent older ESP technology. As mentioned previously, newer technologies are currently available which can improve the removal efficiency of submicron particles. And while over 80% of newly planned units are expected to use scrubber/

fabric filter devices to control particulate emissions, recent industry figures[115,118,119] indicate that less than 50% of the existing MSIs use these newer technologies (scrubber/fabric filter, scrubber/ESP). These statistics also do not include smaller MWI facilities, many of which have no APCS. A recent survey of existing North American MWI capacity, including operating APCS technologies, is given by the National Solid Wastes Management Association.[120,121]

Compared to coal combustion, incineration of municipal solid waste yields much higher concentrations of cadmium and lead in the flyash, and far greater emissions ($\mu g\ m^{-3}$) of arsenic, beryllium, cadmium, and lead,[122] even though peak flame temperatures for coal combustion are likely much higher. Greenberg *et al.*[122] present field data which suggest that many toxic metals are associated with small particles, and that refuse incineration can account for major portions of the antimony, cadmium, and zinc observed in urban aerosols. Law and Gordon[123] attempted to determine which of the emitted metals came from combustible municipal solid waste sources and which came from non-combustible sources (such as scrap metal components, which might be separated before combustion). They concluded that emissions of calcium, copper, mercury, and potassium are likely coming from not easily separable (and often assumed to be combustible) components of refuse. They further concluded that emissions of silver, cadmium, chromium, manganese, lead, tin, and zinc come from non-combustible sources as well as from contributions from combustible materials. They suggest that emissions of aluminium, barium, cobalt, iron, lithium, sodium, nickel, and antimony may be reduced by separating the combustibles from the non-combustibles prior to use as a fuel. However, this kind of comprehensive preseparation is extremely difficult and is often not practical, especially for larger mass burn units. More recently, Korzun and Heck[124] determined that most of the cadmium enters the waste stream with the combustible fraction and can account for a major share of the cadmium observed in flyash and in atmospheric particulates. The most likely sources of cadmium are household batteries, plastics, corrosion-resistant metals, semiconductors, and pigments. Lead emissions appeared to be derived from both combustible and non-combustible discards of batteries, plastics, and pigments. These authors suggest the following fate of cadmium and lead during MWI: of the waste feed, consisting of approximately 9.4 mg cadmium and 992 mg lead per kg of waste (8,500 mg cadmium and 900,000 mg lead per ton of waste), 10.4% of the cadmium and 2.3% of the lead is emitted into the air, 55.2% of the cadmium and 12.6% of the lead is collected as flyash, and 34.4% of the cadmium and 85.1% of the lead is collected with the bottom ash. Equilibrium predictions of the partitioning of toxic metals in a MWI[106] are consistent with these data. One might well expect that this partitioning would depend on a number of factors, not the least of which might be the combustion environment and temperature history. Indeed, Vogg *et al.*[125] state 'the release of various heavy metals in refuse incineration does not depend so much on the concentrations in the refuse itself, but much more on the chemical mechanism acting at high temperatures which, in combination with the non-metallic components present, determine the transfer into the flue gas.' Clearly, the fate of toxic metals as a consequence of incineration processes comprises an important, topical, combustion problem.

Mercury emissions constitute a major technical issue associated with municipal solid waste incineration processes. This has stimulated research on the homogeneous and heterogeneous reaction chemistry of mercury in simulated flue gases,[126] and assessments of how mercury emissions can be controlled.[127,128] Approximately 70% of the total mercury emitted from municipal solid waste incinerators is as mercuric chloride,[125,129] although Hall *et al.*[126] reported a reduction of oxidized mercury to elemental mercury on hot steel surfaces. Injection of Na_2S or powdered activated carbon ahead of dry $Ca(OH)_2$ scrubbers enhanced mercury removal from the flue gas.[128] The use of sulfur impregnated adsorbents for mercury removal has been explored by Otani *et al.*[130,131] In contrast to the use of sorbents in low temperature post flame regions, there is little evidence at this time that high temperature reactive scavenging of mercury by sorbents is effective, although it might be a fruitful area of research.

Toxic and other trace metal emissions from combustion of coal were compared by Norton *et al.*[132,133] to those from 80% coal/20% refuse derived fuel (RDF) mixtures. They concluded that the particulate emissions from firing coal/RDF mixtures are not sufficiently enriched in toxic and trace metallic elements to pose any greater environmental concern than particulate matter from the combustion of coal alone. They found that levels of antimony, cadmium, lead, tin, and zinc in the smaller particle sizes (ESP and stack flyash) were typically less than twice as high in the ash from coal/RDF combustion as found in the ash from coal combustion. Additionally, they found that average levels of antimony, chromium, and lead (along with other trace metals) in the coal/RDF bottom ash were of the order of two to five times higher than those seen in coal bottom ash. These data are significant, since they indicate the possible existence of effective scavenging mechanisms between the coal ash and volatile toxic metals from the RDF.[132,133]

Hospital or medical waste incinerators are often considered to represent a class of MWIs. However, even though similarities exist between hospital and municipal waste incinerator designs, there are also significant differences. Hospital wastes contain approximately 85% general refuse with the remaining

15% contaminated with infectious agents.[134] Hospital wastes contain approximately 20% plastic (most commonly polyethylene, polypropylene, and polyvinyl chloride) by weight, which is approximately four times the amount found in municipal wastes.[134] Hospital waste is often burned in smaller units than municipal waste with less sophisticated APCSs.[135] Kauppinen and Pakkanen[135] examined the elemental size distributions of aerosols produced from a Hogfors hospital waste incinerator. They reported the formation of a bimodal size distribution with large fractions of the measured sulfur (>90%), zinc (20–80%), cadmium (62–77%), and lead (7–74%) found in the fine mode (0.1–0.2 μm). They also report that aluminum, iron, magnesium, and titanium were found only in the coarse mode (6–10 μm). They attribute the existence of the fine mode as an indication that at least part of these elements vaporize during the incineration process. Compared to other MWIs, medical waste incinerators are likely to have notably higher mercury emissions.

In concluding this section, it should also be mentioned that, in the exhaust gases of MWIs, some trace metals, especially copper chlorides, have been implicated in playing critical roles in the *de novo* synthesis of PCDDs and PCDFs.[24–32] However, detailed review of this important subject is outside the scope of this paper.

3.2.5. *Industrial processes and sewage sludge*

Cement and other mineral processing kilns would appear to be useful combustion devices for the destruction of hazardous materials. Temperatures are high, excess oxygen is present, and residence times are long. Furthermore, although questions remain concerning the use of products derived from hazardous wastes, the potential exists for immobilizing toxic metals in the process products. This facet has been investigated by Cartledge *et al.*[136] who found that, in cold non-combustion processes, cadmium could be trapped to form water unleachable compounds while the isolation of lead was less successful. Gossman[137] presented data on the fate of toxic metals introduced with hazardous waste fuels and other raw materials into wet, portland cement kilns, and found that arsenic, cadmium, lead, mercury, selenium, and thallium tend to concentrate in the kiln dust, although arsenic, lead, and selenium will also exit with the product clinker (bottoms). Surprisingly, 95% of the antimony (a volatile metal) exited the process with the clinker, at least for one kiln. More research could be of value in understanding and predicting the fate of toxic metals during high temperature mineral processing, and in examining the safety and long term stability of products manufactured when hazardous wastes are used.

The size classified characterization of metal emissions from a primary zinc/lead smelter has been reported by Harrison and Williams.[138] Size segregation was accomplished using a 30 lpm Andersen cascade impactor with a minimum aerodynamic particle size cut of 0.43 μm in diameter (collected by the after filter). In general, 50% of the mass of cadmium, lead, and zinc particles was contained in particle sizes less than 1 μm in diameter. The high temperature environment in the smelter was not described.

Sewage sludge contains significant levels of arsenic, cadmium, chromium, lead, and nickel,[139] and is often incinerated using a wide range of combustion devices, including multiple hearth incinerators, fluidized bed incinerators, and sometimes cement kilns. Bennett and Knapp[140] characterized air emissions and measured particle size distributions for cadmium, calcium, iron, and zinc. Cadmium and zinc contributed to a significant submicron mode at approximately 0.2 μm in diameter. Dewling *et al.*[141] found that 1% of the chromium, copper, lead, and zinc passed through the scrubber and was emitted from the stack of a fluidized bed sewage sludge incinerator. Interestingly, cadmium (a volatile metal) was entirely accounted for in the collected ash or in the scrubber water. The partitioning of cadmium, chromium, copper, lead, mercury, nickel, and zinc during the slow pyrolysis of sludge (up to 750°C) was investigated by Kistler *et al.*[142] They found that chromium, copper, lead, nickel, and zinc were retained quantitatively in the char at temperatures up to 750°C. Cadmium was volatilized at temperatures greater than 600 °C, and mercury was volatilized at the lowest temperature investigated (350°C). The metals retained in the char were highly immobile to leaching, and this was attributed to the alkaline nature of the ash, which tended to neutralize acidic leaching water.

4. MECHANISM OVERVIEW

The preceding discussion on the occurrence of toxic metals in combustion and incineration processes has highlighted both the large variety of methods by which toxic metals may be introduced into the combustion chamber, and the range of combustion environments in which the metals are subsequently processed. Of interest here is to determine the extent to which these variations affect the subsequent transformation of the metal before it leaves the process (see Fig. 1). The overriding question is whether the metal will leave the combustor as vapor or as submicron particles, which are difficult to collect and isolate from the air environment, or whether it will form or combine with easily collectable large ash particles, which may, either with or without further treatment, be isolated from the aquatic and soil environments. Omitted in the discussion that follows are mechanisms occurring within or on deposits or heat transfer surfaces inside boilers or furnaces, since these have been well covered in the 'fouling and slagging' literature (see Raask[39]).

We have shown that metals may be contained in

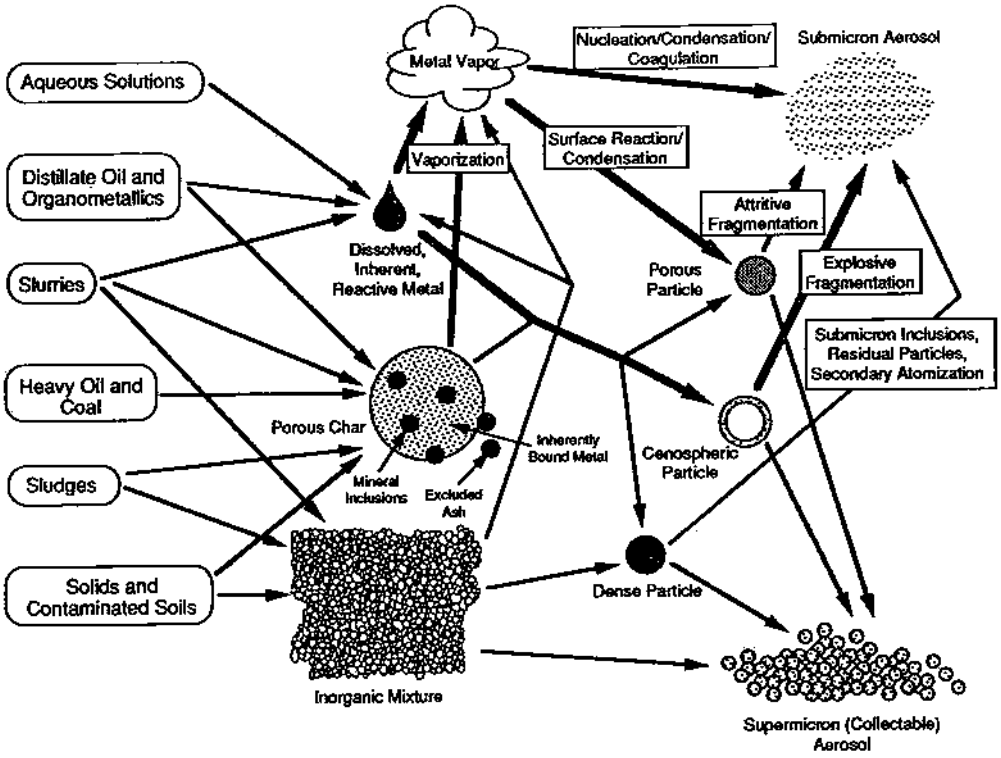

FIG. 4. Possible controlling mechanisms for particle formation in combustion systems.

solid or liquid fuels, chemically bound to the organic fuel matrix (inherent mineral matter), or dispersed within the solid fuel particle as mineral crystallites (included mineral matter), or indeed, completely extraneous to the fuel particle (excluded mineral matter). Alternatively, toxic metals may be chemically bound within organometallic compounds such as chelates or physically mixed, as in paints, pigments, and solvents. They may enter together with other inorganic clays and soils, as during the thermal treatment of contaminated soils,[143] or they may be contained in aqueous solutions and sludges. Toxic metals may be introduced into a combustion environment continuously through atomizers,[144] lances, or screw feeders, or through entrance chutes in a batch mode as solids or contained liquids. They may be introduced into the combustion chamber as single salts or individual compounds, or they may enter as mixtures. A critical issue in designing test burns for incinerators is whether the form in which the metal is introduced is representative of the behavior of other forms of that metal. The left-hand side of Fig. 4 represents some of the various forms in which a metal-containing waste may be introduced into a combustor, and how this physical state can influence the ultimate fate of that metal.

Upon entry into the incinerator, the metals contained in the waste stream are transformed into various physical forms. Dissolved metal salts, such as nitrates or pyrites, may form reactive metal compounds which may decompose violently at elevated temperatures. They may also decompose as viscous melts to form cenospheres which can burst into submicron fragments.[145] Alternatively, the metal compound may be confined within a porous char matrix. This will happen, for example, to inherent (organically bound) metals in heavy oil or both inherent and included mineral matter in pulverized coal. The metal must then be released either within the matrix, subsequently to diffuse through it, or it will enter the gas phase as the char matrix itself is oxidized. In the event of the former process, there is the opportunity for the metal to react with included silicates to form stable compounds which fail to vaporize. Alternatively, the metal which has been released may diffuse back into the char matrix remaining, to react with included silicates situated there, or it may react with excluded silicate particles in the disperse phase. Finally, one metal (e.g. sodium) may displace another metal (e.g. potassium) which would otherwise be immobile and bound in a stable mineral form, such as illite. Mineral inclusions may also coalesce as the carbon matrix recedes to form particles larger than the individual inclusions. The physico-chemical processes involved in the release of toxic metals may thus be quite complex. It may be kinetically controlled, and the overall amount of a toxic metal released may, under certain circumstances, have little to do with equilibrium.

When a metal contained in contaminated soils, sludges, or slurries is introduced into an incineration environment, an inorganic mixture containing both

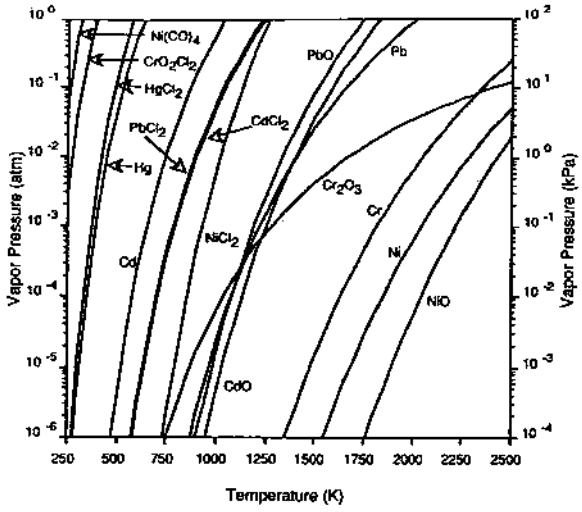

FIG. 5. Vapor pressure vs temperature for selected metal compounds.

the toxic metal and potential scavenging agents, such as clays and glasses, is formed. It is not surprising, therefore, that (upon heating) much of the toxic metal will react with the clay and only a little will be released to form a condensable vapor. This has been experimentally confirmed for lead/montmorillonite clay mixtures by Eddings and Lighty.[143] Their study showed large deviations from simple equilibria based on selected pure condensed phases, during the heating of inorganic mixtures. The work of Queneau *et al.*[33] addresses the thermodynamics of the vitrified mixtures likely to be formed under these conditions, and is useful where inorganic mixtures are formed, as shown in Fig. 4.

The primary physical forms of the toxic metals outlined above (reactive metal compounds, porous chars, and inorganic mixtures as shown in Fig. 4) can then undergo further transformations to other physical forms including metal vapors, porous metal ash particles, cenospheric (hollow) ash particles, or dense ash particles. Upon cooling, the supersaturated vapor may condense on the surfaces of existing particles, or if sufficient surface area is not available, homogeneously nucleate to form tiny particles. These particles will subsequently collide and coagulate as described in Section 6. Alternatively, there is evidence that a metal vapor may *react* on the surface of existing particles or sorbents. In contrast to the first two processes (heterogeneous condensation and homogeneous nucleation), surface reaction does not require the metals' partial pressures to exceed their vapor pressures. These mechanisms and processes strongly influence the chemical and physical form in which the toxic metal under consideration enters the environment. They are likely to depend strongly on the combustion environment and temperature history experienced by the metal compound, as well as on the initial form in which it is introduced into the combustion chamber, and on the presence or absence of other species in the mixture.

The mechanisms depicted by the bold arrows in Fig. 4 will now be examined in more detail. The objective is to determine how well we can predict the partitioning of metals between the various physical forms shown in Fig. 4, and the various chemical forms in which each metal can appear.

5. PARTITIONING OF METALS TO FORM AIRBORNE PARTICLES

The formation of submicron particles containing toxic metals is a major issue in the incineration of nearly all metal containing wastes. This section addresses this issue both theoretically and experimentally. Theoretical arguments are based on equilibrium predictions, which are limited to determining the expected concentrations of only those species for which accurate thermodynamic data are available. Equilibrium predictions may be quite incorrect if important species are omitted from the calculation. For example, the hexavalent chromium species, $CrO_2(OH)_2$, is not included in the calculations presented here, although very recent results[146] suggest it may be important under selected conditions. Kinetic limitations may also prevent these equilibrium predictions from being followed in practice. For these reasons, it is imprudent to rely excessively on equilibrium predictions, which may not necessarily follow experimental data. Equilibria, however, do provide the first step in gaining insight into the behavior of complicated processes, and for this reason we discuss them in some detail here.

Experimental results are presented in two parts. First, we discuss metal release and small particle formation from various pure metal compounds. Second, we explore data on metal release and subsequent small particle formation from mixtures of metals. For the latter we draw on the considerable body of data available on the fate of volatile metals during coal and coal char combustion, where the volatile metals are initially present in a char matrix in close proximity to one another and to other inorganic species such as silicon. As a practical matter, therefore, this section of the paper addresses the issue of how the *initial form* of the metal might influence its initial partitioning between bottom ash and airborne particulates.

5.1. *Theoretical Predictions: Equilibria, Vaporization and Condensation of Metal Compounds*

As shown in Fig. 4, a likely, but not the only, mechanism for the formation of small particles enriched in toxic metals, is through the high temperature vaporization of the toxic metal constituents either as introduced, or after transformation within the combustor, followed by condensation of the

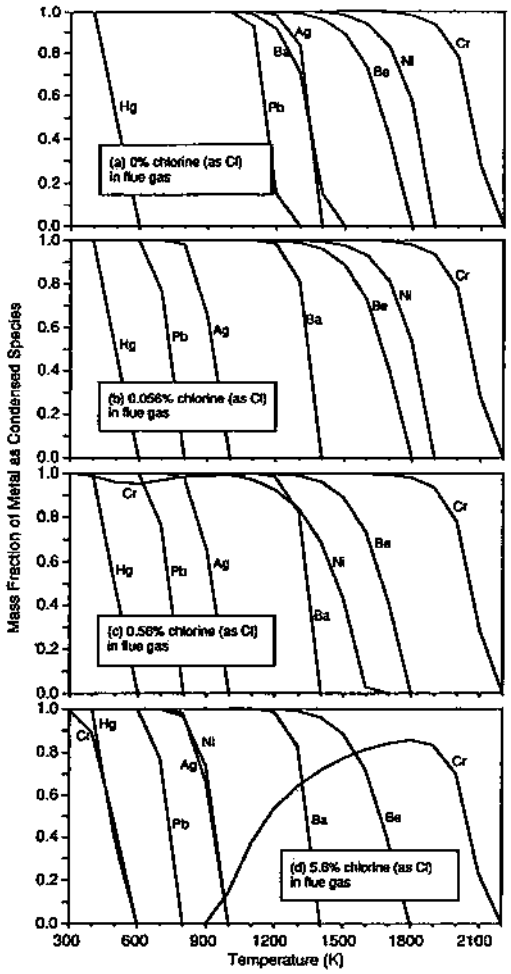

FIG. 6. Equilibrium predictions of condensed metal species as a function of temperature in a simulated flue gas environment with (a) metal only (0% mol Cl), (b) chlorine/metal ratio of 1/1 (0.056% mol Cl), (c) chlorine/metal ratio of 10/1 (0.56% mol Cl), and (d) chlorine/metal ratio of 100/1 (5.6% mol Cl).

supersaturated vapor either around existing particles or forming tiny nuclei of the metal (compound) itself. To address this mechanistic route, we consider first the vapor pressures of selected toxic metal compounds, since this provides a guide to their potential volatility.

Figure 5 depicts the vapor pressure of several toxic metal compounds as a function of temperature. Nickel and nickel oxides have relatively low vapor pressures, even at high combustion temperatures. Therefore, they should not be expected to be easily vaporized. $NiCl_2$ and $Ni(CO)_4$, however, have very high vapor pressures at combustion temperatures. Therefore, these compounds are expected to be easily vaporized. Cadmium, lead, and their oxides would also be expected to vaporize in combustion environments. In general, chlorides of all metals have high vapor pressures, when compared to their corresponding oxides. Therefore, the presence of chlorine is predicted to enhance metal vaporization. Mercury has appreciable vapor pressures even at ambient temperatures, and the high volatility of CrO_2Cl_2 (a hexavalent form) is especially noteworthy.

Vapor pressures of pure compounds, however, do not show which species are favored according to equilibrium considerations, and do not by themselves, predict when and under what conditions condensation will occur. Figures 6a, b, and c present results from multicomponent equilibria predictions made by the NASA CET89 computer code.[147] This code calculates equilibria between a given list of species, and allows only ideal gas mixtures and pure condensed species. The solutions obtained depend on the species for which thermodynamic data are included, and if an important species containing the element in question is omitted, the prediction will be quite incorrect. The calculated solutions also may depend on the mix of metal elements which are introduced in the initial mixture. For the results presented here, we have included barium, beryllium, chromium, lead, mercury, nickel, and silver, but were unable to find all the necessary data for antimony, arsenic, cadmium, selenium, and thallium, which are, therefore, excluded. The fate of approximately 80 ppm of each metal in the flue gas resulting from combustion of methane at a stoichiometric ratio (SR) of 1.2 was investigated. The model used here does not allow non-ideal condensed solutions (such as complex slags and glasses, which are known to be formed),[33] although such models are becoming available and might be used in future work. Figures 6a, b, c, and d present the fraction of an element present as a sum of all condensed species vs temperature. Figure 6a shows results without chlorine. Excluded in this calculation are species involving more than one metal, such as $NiCr_2O_4$ (solid) which at temperatures below 1900 K was predicted to contain half the nickel and all the chromium when both metals are present. The species NiO_2H_2 is responsible for keeping nickel in the vapor phase until a temperature of 1800 K is reached. If NiO_2H_2 were omitted from the calculation, nickel would be in the condensed phase over the entire temperature range considered here. Addition of chlorine complicates the results considerably. First, there is competition for chlorine between hydrogen (from water of combustion) and the metals, taken as a whole. Second, there is competition for chlorine between the various metal species. For example, barium, lead, and silver have a greater affinity for chlorine than do beryllium, chromium, and nickel. Therefore, it is instructive to examine the effect of various amounts of chlorine on the fate of each metal in the metal mixture. Figure 6b presents results for 80 ppm of each of the seven metals in the flue gas, with the addition of sufficient chlorine to total approximately 560 ppm chlorine (atom) in the flue gas (primarily as HCl when no metals were present), or at a molar chlorine/sum of all metal ratio of 1. This represents the fate of metals when

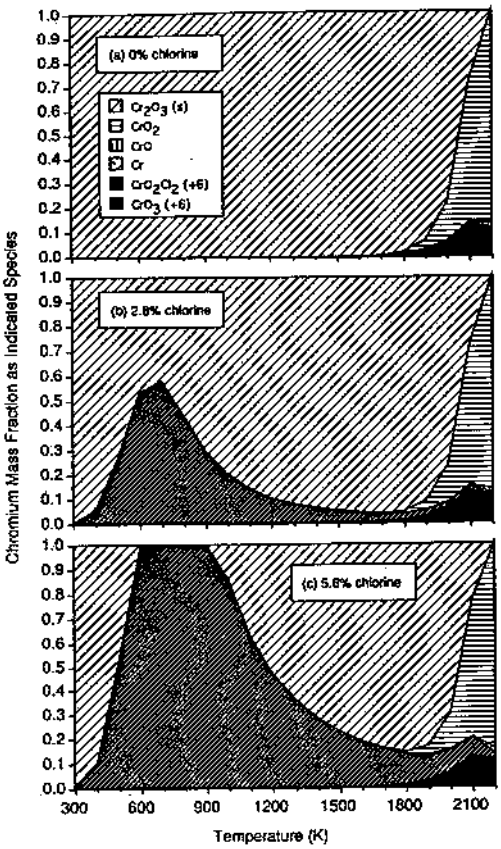

FIG. 7. Equilibrium predictions of chromium valence as a function of temperature in a simulated flue gas environment with (a) metal only (0% mol Cl), (b) chlorine/metal ratio of 50/1 (2.8% mol Cl), and (c) chlorine/metal ratio of 100/1 (5.6% mol Cl).

there is only a trace of chlorine available. In Fig. 6c, 10 times more chlorine has been added, to total 5,600 ppm chlorine (atom) in the flue gas, or a molar ratio of chlorine/(sum of all metals) ratio of 10. In Fig. 6d, the amount of chlorine has been multiplied by 10 again, to total 5.6% chlorine (atom) by volume in the flue gas, or a chlorine/(sum of all metals ratio) of 100. This leads to 5.6% HCl in flue gas at 1600 K in the absence of metals, and this high concentration of chlorine in an incinerator flue gas prior to acid gas control is not unusual in practice, and in fact may be much higher. For all calculations involving chlorine, the species $PbCl_4$ (gas) was omitted, since it was otherwise predicted to be the dominant lead species even at room temperatures, and this has not been observed experimentally.[143,148]

In general, chlorine delays condensation of all species, but low levels of chlorine affect the condensation of lead and silver preferentially to that of beryllium, chromium, and nickel. Even a tiny amount of chlorine changes the speciation of the condensed barium species from the oxide to the chloride, but the temperature at which condensation occurs is affected only slightly due to the narrow spread in the boiling points of the two species. The effect of chlorine on the fate of mercury is slight, with the mercury condensing at approximately 500 K for all cases. The effect of chlorine on the fate of lead is quite profound. Figures 6a through 6d show that even relatively small amounts of chlorine keep lead in the vapor form (as $PbCl_2$) until much cooler regions of the combustor are reached. In fact, if the species $PbCl_4$ were also considered as a possible species in the equilibrium calculation, then predictions would allow all of the lead to remain as a vapor at temperatures as low as 250 K. However, Eddings and Lighty[143] noted the absence of $PbCl_4$ in their experimental samples. Chromium behavior is especially interesting, since there is a narrow temperature window around 700 K, within which CrO_2Cl_2 (gas) is thermodynamically predicted to appear, while on either side of the window, condensed forms of chromium are favored. CrO_2Cl_2 dissociates at temperatures that are below those at which the condensed form is favored. Because of the importance of chromium speciation (trivalent vs hexavalent), this element is discussed in more detail below. Nickel condensation is also affected by the presence of chlorine, but, compared to lead, the effect is less notable until higher chlorine levels are available. In all cases, the effect (if any) of chlorine is to lower the temperature at which there is a transition between vapor and condensed toxic metal species. For combustion systems, this implies that chlorine will enhance the vaporization of metals at low temperatures, and subsequently delay their nucleation and condensation.

The speciation of chromium compounds is extremely important. Hexavalent chromium (Cr^{6+}) is considered a potent carcinogen at low concentrations, while trivalent chromium (Cr^{3+}) has a higher toxicity threshold. Figure 7 shows equilibrium predictions of chromium species as a function of temperature and chlorine concentration in the flue gas. Results are for approximately 80 ppm chromium in the flue gas, and were obtained when other metals (namely 80 ppm of each of barium, beryllium, lead, mercury, nickel, and silver) are also present. Large amounts of chlorine, totaling 2.8% by volume in the flue gas, are required before significant chlorination of chromium appears. In Fig. 7, the fractions of total chromium present as the two hexavalent chromium species (CrO_3 and CrO_2Cl_2) are denoted by the two darker shadings. Of special interest is the predicted effect of chlorine concentration. A small fraction of the hexavalent CrO_3 is formed at high temperatures under all chlorine conditions. However, Fig. 7 suggests that high chlorine levels might promote the formation of the carcinogenic hexavalent CrO_2Cl_2 in a temperature window around 700 K (i.e. in the post-combustion zone). Again, it should be emphasized that the equilibrium predictions may not be realized if either other chromium species not considered in this calculation are important, or kinetic rates are too slow to allow equilibrium to be reached. Homogeneous kinetics may well be insufficiently

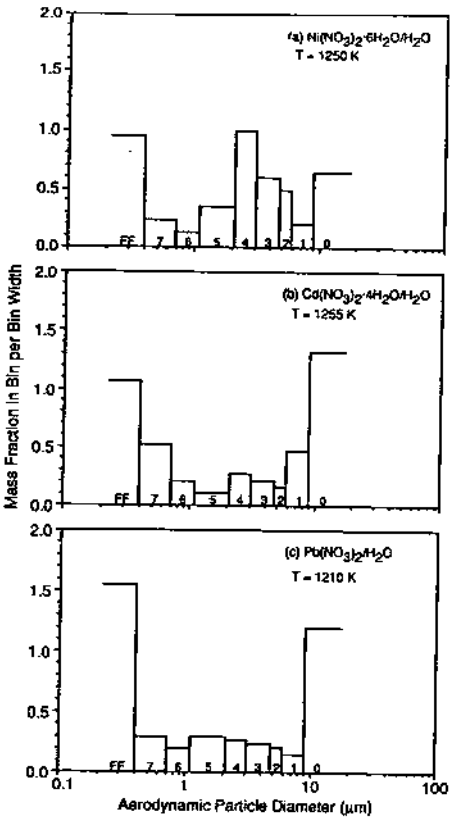

FIG. 8. Particle size distributions (a) of nickel, (b) cadmium, and (c) lead nitrates from a laboratory drop tube furnace (adapted from Mulholland and Sarofim[145]).

rapid at these low temperatures to form this hexavalent species, but catalytic reactions forming hexavalent chromium in the presence of chlorine should not be ruled out. These results suggest that, if hexavalent chromium is found in incinerator exhausts, in the presence of chlorine, it may be worthwhile to determine if it might be formed in hot particulate control devices, where catalytic processes, forming PCDD and PCDF compounds for example, have been shown to occur.

We have also completed equilibrium calculations in which the effects of sulfur alone, and sulfur in the presence of chlorine, were each examined. Apparently, sulfur has little effect on the condensation temperature of most of the indicated species, although it does change the nature of the condensed species at low temperatures. In the case of 80 ppm lead in the flue gas, sulfur without chlorine can lower the condensation temperature from 1200 K to 1000 K, due to the sulfation of the lead oxide. In the presence of chlorine, the major effect of sulfur is to *raise* the lead dewpoint by about 200 K, because the sulfate is favored over the chloride at the higher temperatures. Especially intriguing is the effect of sulfur on the yield of hexavalent chromium compounds. As shown in Fig. 7, equilibrium, with about 5 volume % chlorine in the flue gas, predicts 100% conversion of chromium to hexavalent CrO_2Cl_2, in a fairly broad temperature window (1000–600 K). If we add sulfur in an amount to equal the chlorine, the maximum yield of hexavalent chromium is restricted to 71%, and this occurs in a very narrow temperature window at 900 K. At 800 K, $Cr_2(SO_4)_3$ condenses and removes chromium from the system in trivalent form. Thus, the effect of sulfur in combination with chlorine is, in some cases, to inhibit the formation of volatile metal chlorides, and thus to raise dewpoints relative to the case with an excess of chlorine alone.

5.2. *Experimental Data on Metal Partitioning to Form Airborne Particles*

Results from two scales of laboratory experimentation are presented. These consist of a bench scale drop tube, in which the behavior of individual particles can be observed, and a downflow laboratory combustor, in which combustion is self sustaining, and particle densities and particle/gas environments are designed to simulate more practical configurations. Discussion focuses on two broad aspects of the problem: first, the partitioning of metals when released into the combustion chamber as pure metal compounds, and second, the effects of the metals being introduced into the combustion chamber mixed with other compounds. The metal being released may initially be in a mineral form, bound into a char or carbonaceous compound, or in contact with other inorganic compounds such as silicon. The potential for metal/metal interactions is also explored.

5.2.1. *Pure metal compounds*

Drop tube data were obtained by Mulholland and Sarofim[145] and Mulholland *et al.*,[149] who investigated the formation of small particles from aqueous solutions of cadmium, lead, and nickel nitrate salts, which were injected into a hot nitrogen/oxygen environment in an externally heated tube, as a monodisperse droplet (36 μm diameter) stream. The experiment was well controlled and isothermal. Resulting particle size distributions are shown in Fig. 8. These data are significant, since they show a strong submicron mode for the nickel salt which, according to the equilibrium predictions in Figs 5 and 6, is not expected to vaporize at temperatures as low as those examined experimentally (1250 K). Consequently, vaporization and subsequent nucleation of nickel salt can be ruled out, and it is necessary to propose some other mechanism for the formation of the submicron particle size mode shown. Furthermore, Fig. 8 shows three distinct modes for each metal, with the middle mode especially pronounced for the nickel salt. Mullholland and Sarofim[145] show that the submicron mode for nickel was formed as a consequence of the explosive fragmentation of

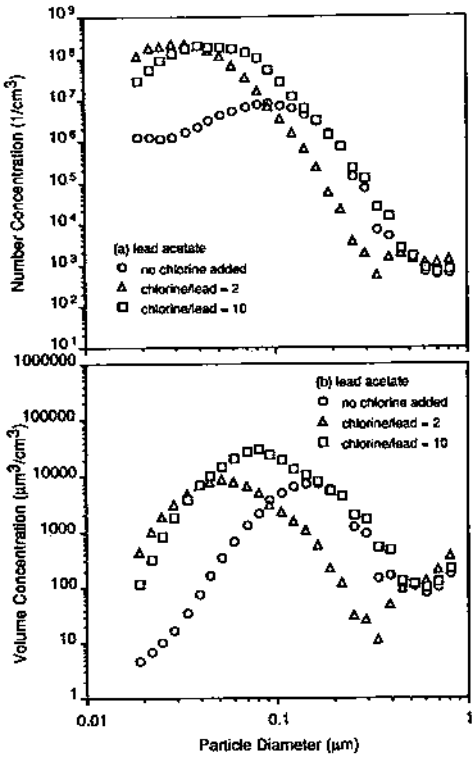

FIG. 9. Effect of chlorine addition on the lead submicron number and volume particle size distributions in a laboratory combustor (adapted from Scotto *et al.*[148]).

cenospheres. They conclude that the middle (1.0–7.0 μm) mode was the result of the aerodynamic classification of larger low density cenospheres, and the residual (7.0 μm) mode was due to dense (unreacted) residual metal particles (one per droplet). Nitrates of lead and cadmium also decompose. Lead nitrate decomposes by sublimation, and this produces porous particles of varying density to form the intermediate mode for that compound. Cadmium nitrate decomposes as a low viscosity liquid and forms dense particles with almost no intermediate particle size mode. Submicron particle formation of cadmium and lead is in qualitative agreement with mechanisms involving vaporization of cadmium and lead. The existence of a non-vaporization mechanism for the formation of submicron particles from certain metal compounds [such as $Ni(NO_3)_2$] is significant, since it indicates that the initial speciation of the metal plays a role in its subsequent fate. A different nickel salt or compound, for example, might well fail to form cenospheres, and therefore, fail to explosively fragment. Conversely, the existence of a submicron mode does not necessarily indicate that the metal has passed through a vaporization/nucleation/condensation process. Mulholland and Sarofim showed also that increasing temperature enhanced the submicron particle size for lead and cadmium, but had little effect on that for nickel. Clearly, submicron particle formation due to vaporization followed by nucleation and condensation in the sampling probe is promoted by high furnace temperatures.

Figure 9 presents particle number and volume size distribution data of a lead aerosol effluent from a 17 kW, 0.15 m I.D., insulated downflow combustor in which an aqueous solution of lead acetate was sprayed through a self sustained natural gas flame.[148,150] Particles were sampled through a doubly diluted isokinetic sampling probe and delivered to a differential mobility particle sizer (DMPS) in conjunction with a condensation nuclei counter to determine the particle size distribution. Open circles represent a particle size distribution taken without the addition of chlorine, and open triangles represent data taken with a chlorine/lead molar ratio of 2. These particles are very small, with a peak in the volume distribution at approximately 0.2 μm diameter (0.08 μm in the presence of chlorine), and it can be seen that the presence of chlorine influences the particle size distribution measured. $PbCl_2$ is much more volatile than the oxide (see Fig. 5), and the effect of this is to delay condensation/nucleation until after cooling and dilution in the probe. Without chlorine, the particle size distribution has evolved (by coagulation) inside the furnace, while in the presence of chlorine, the lead formed an aerosol later in the furnace or was initially sampled as a vapor, and then dilution and rapid cooling in the probe caused nucleation. This resulted in a younger (less evolved) particle size distribution. The important thing to note is that the addition of chlorine leads to sampling a less coagulated, less mature, lead aerosol, which contains a larger fraction of very small (<0.1 μm) particles. This occurs because chlorine delays the condensation of the metal, and lowers the dewpoint (see Fig. 5).

5.2.2. *Mixtures*

Mixtures can exert a profound effect on the initial partitioning of volatile metals. Eddings and Lighty[143] showed that when lead deposited on clay was heated in a bed between two screens, significant deviations from equilibrium occurred and appreciable quantities of the metal failed to vaporize. Indeed, based on the solution equilibria presented by Queneau *et al.*,[33] one might expect that lead would react with the alumino-silicate compounds present in the clay. As will be shown later, this facet can be exploited to help control airborne lead emissions.

The behavior of a volatile metal which is initially bound in a *char matrix* in close proximity to other inorganic minerals can best be examined by revisiting the release of sodium initially bound in coal (discussed briefly in Section 4). Clearly, sodium is not an identified toxic metal (see Table 1), nor is a coal or coal char the most common physical form in which a metal is introduced into an incinerator. However, examination of the fate of a volatile metal such as sodium in particle environments, such as a char,

TABLE 9. Concentrations of inorganic elements (as major oxide) in the ash of two coals (adapted from Gallagher[158])

Weight percent	Beulah lignite	Loy Yang
SiO_2	21.6	7.56
Al_2O_3	14.5	2.05
TiO_2	0.0	0.005
Fe_2O_3	12.2	3.61
CaO	17.1	2.72
MgO	4.2	12.9
P_2O_5	0.0	na
Na_2O	6.1	28.14
K_2O	0.3	<0.5
SO_3	21.1	12.08
Cl	na*	30.91
Percent ash in coal	13.81	2.44

*Not available.

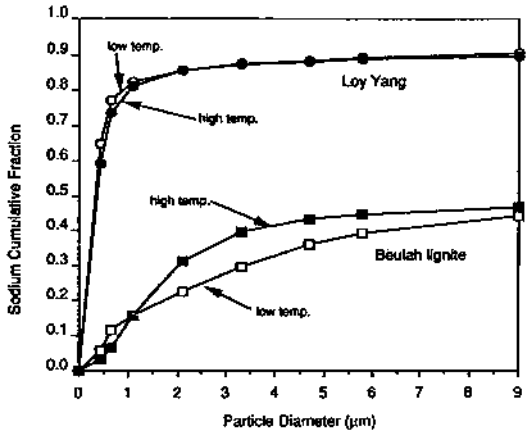

FIG. 10. Comparison of sodium cumulative fraction as a function of particle size for flyash samples from Loy Yang and Beulah lignite coals (adapted from Gallagher *et al.*[40]).

does provide useful information on how the physical and chemical forms of both the metal and contiguous neighboring species influence the release of the metal into the vapor phase.

The release of potassium and sodium during coal combustion has been studied by a number of investigators,[40,151-158] and may shed light on what might be expected for toxic metals organically bound in the coal char or solid phase of other fuels or wastes. Furthermore, studies on silica ash vaporization from synthetic chars[159] yield information on the importance (or lack of importance) of reducing reactions in this process. Organically bound metals, such as sodium bound to the carbon atoms in char, are released at temperatures far in excess of those at which sodium salts, oxides, and hydroxides devolatilize.[41] In fact, during coal char combustion, organic sodium release may not occur until char burnout is well under way. Thus, the vaporization of sodium under these circumstances has little to do with the vapor pressures of sodium salts. Sodium or potassium, originally bound in minerals, such as silicates, alumino-silicates, or illites, would not be expected to vaporize at combustion temperatures but, as we shall see presently, potassium can be displaced by certain metals.

Considerable insight can be obtained by comparing the behavior of sodium released during the combustion of two very different coals. Gallagher[158] examined two coals including a low rank Australian coal (Loy Yang) and a low rank North American coal (Beulah lignite). Table 9 summarizes the mineral matter content for each of these coals. The Beulah lignite contains significant amounts of both sodium and silicon in the mineral matter, while the Loy Yang has sodium present with very little associated silicon. The total amount of sodium in the Beulah lignite is greater than that in the Loy Yang, although in both cases the majority of the sodium is acid soluble, meaning that it is *not* already bound (as in nephalite) with silicon and aluminum. Although the Loy Yang contains significant amounts of chlorine, the sodium is not present as raw sodium chloride. Srinivasachar *et al.*[43] have showed that, while chlorine is released rapidly at low temperatures (approximately 1000 K), the sodium for *both* the Loy Yang and the Beulah lignite is released at much higher temperatures (1800 K). Figure 10 presents the fraction of the total sodium ultimately found in sampled ash particles up to 9 μm in diameter.[40] If we assume that sodium in particles less than 0.7 μm originated from a vaporization/condensation mechanism, then we can conclude that, while over 80% of the Loy Yang sodium passes through this mechanism, less than 12% of the Beulah lignite sodium suffers the same fate. This 0.7 μm particle size might seem arbitrary; however, Section 6 will show that small combustion nuclei tend to accumulate (by coagulation) into a size range of approximately 0.5–1.0 μm. Furthermore, while the fate of sodium from the Loy Yang is roughly independent of temperature, vaporization of sodium from Beulah lignite *decreases* with increasing temperature. That is, higher temperatures cause more of the sodium to be shifted toward the larger particles. Other data[157] showed that some of the sodium ultimately appeared as a sodium alumino-silicate ($NaSiO_2Al_2O_3$). Thus, the release of sodium into the vapor is governed by a competition between the mechanisms promoting release and those promoting capture by alumino-silicates. Gallagher[158] has shown that the release of sodium, and its subsequent capture by silicon depend on temperature in various, complicated ways. Organic sodium is released into the gas phase by two mechanisms: first, through release (vaporization) inside the char particle with subsequent diffusion to the outside and second, through release at the outer layers of the char particle as the neighboring carbon atoms are oxidized to form gaseous species. When the char oxidation reactions have a weak temperature dependence (film diffusion controlled regime), the amount of sodium ultimately able to condense from a vapor in the combustor will decrease with increasing temperature. This is because the sodium release process then has a

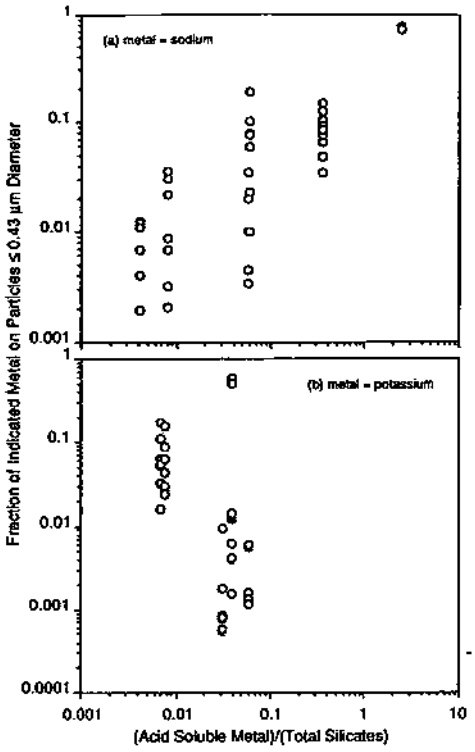

FIG. 11. Comparison of sodium and potassium vaporization as a function of total silicate concentration of various coals (adapted from Gallagher *et al.*[40]).

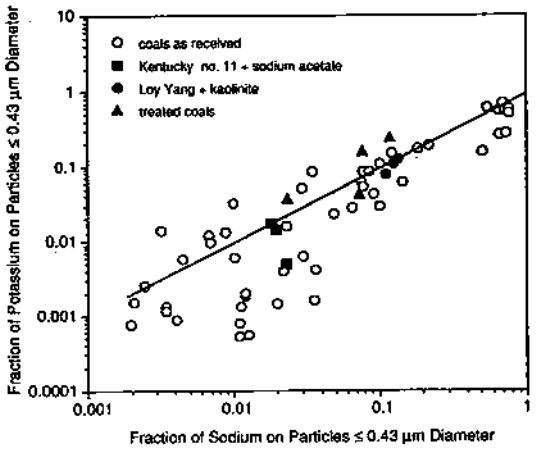

FIG. 12. Comparison of mass fraction of sodium vs potassium on an impactor after filter (particle diameter $\leq 0.43\ \mu m$) for various coals (adapted from Gallagher *et al.*[40])

weaker temperature dependence than the sodium capture process.[153,160] When, on the other hand, char burnout has a high activation energy (pore diffusion controlled or kinetic controlled regime), the overall sodium release mechanism has a higher activation energy than the capture mechanism, and the amount ultimately able to condense from the gas phase increases with increasing temperature.[158] Thus, there is an interaction between char burnout kinetics and the temperature dependence of sodium released. For the Beulah lignite, the capture mechanisms have higher activation energies than the release mechanisms; therefore, the fraction of sodium captured will increase with temperature. The Loy Yang contains minimal quantities of alumino-silicates to capture sodium; therefore, the amount released into the vapor is not dependent on temperature. It is possible that for other coals, the overall release rate of sodium from the char may have a higher activation energy than that for the sodium capture reaction, in which case the overall temperature dependence of the net amount of sodium released will be opposite to that observed for the Beulah lignite.

These results suggest that the fate of sodium, and possibly other volatile toxic metals, is determined in part, by its proximity to alumino-silicate compounds. Figure 11a[40] shows that for numerous coals, the fraction of sodium ultimately found in the small particle size range ($< 0.43\ \mu m$ diameter, and assumably previously vaporized) can be correlated with the ratio of acid soluble sodium divided by the amount of total silicates. The size of the silicate inclusions may also be important, since surface area may influence the flux of alkali to the inclusions during burnout.[158] Clearly, the presence of silicates together with a vaporizable metal has a great influence on the fraction of that metal which enters the gas phase and ultimately nucleates or otherwise contributes to form submicron particles in the exhaust.

The discussion above has been restricted to *acid soluble* sodium; that is, organically bound alkali which would be expected to be released into the gas phase at combustion temperatures. One might expect that similar mechanisms might be used to describe the fate of potassium, but this is not the case, as shown on Fig. 11b. Unlike sodium, the release of potassium does not correlate with the acid soluble portion of that constituent divided by total silicates. However, the fraction of potassium vaporized does correlate with the fraction of sodium vaporized as shown on Fig. 12. Here, appreciable amounts of potassium originally bound with silicates (as illite) is unexpectedly released to form small particles. It would appear that mobile sodium is able to displace mineral bound potassium, which would not otherwise be expected to vaporize. Bench scale studies[158] have confirmed that this occurs when both sodium and chlorine are available in the gas phase, but not in the absence of either one of these constituents. The significance of these data to the fate of toxic metals is that it might be unwise to assume that once a metal is bound to a silicate it must remain bound there forever. These data suggest that such a bound metal can be displaced, and mobilized, by another metal vapor. Whether this same phenomenon occurs with toxic metals is not yet known, but could be the subject of future research. For example, it might be interesting to extend the studies of Eddings and Lighty[143] to examine the vaporization of lead from

a lead/montmorillonite clay mixture, both in the absence and presence of sodium and chlorine.

Recent results[161] suggest similar (limited) lead release from nitrates, chlorides, and sulfates which were dissolved in water with trace organic contamination, and adsorbed on montmorillonite clay sorbent. The purpose of these experiments was to investigate metal release during the thermal treatment of soils. Substantial release of cadmium and copper were observed, but the initial speciation did not seem to be important in these experiments, where large amounts of sorbent-like material were always available. Work on the release of various metals from contaminated soils is continuing.

5.2.3. *Summary*

Clearly, the vaporization and release of 'volatile' metals is not completely determined by the vapor pressure of a few simple species containing that metal, although that information is helpful especially regarding the possible influence of chlorine. The overall metal release process may become quite complex when metals are present together, when they are associated with silicon compounds, or when they are chemically bound within a char matrix. Release then involves complicated chemistry between the inorganic species, and is coupled to the oxidation rate of the organic char, if present. Equilibrium predictions alone may be very misleading, since the initial speciation of the metal is clearly very important (note the reliance on 'acid soluble' to denote 'potentially mobile' sodium for the coals). Additionally, the presence or absence of nearby alumino-silicates, the presence or absence of other metal species, and chlorine can all play a role. The laboratory combustor data on lead particle size distributions both with and without chlorine present (Fig. 9) clearly illustrate the need to understand not only how the metal may vaporize, nucleate, condense, or otherwise form small particles, but also how that particle size distribution might evolve as it is carried through the combustor SCC, and to the APCS. This is the subject of the next section.

6. AEROSOL DYNAMICS IN THE COMBUSTION CHAMBER

Aerosols are suspensions of liquid or solid particles in gases. Aerosol particle sizes range from nanometers to tens of micrometers. The previous discussion has shown that the impact of metals on the environment is determined in part by the metal aerosol particle size distribution (psd). Depending on the time/temperature history, combustion environment, and the presence of other constituents, many metals will vaporize at high temperatures near the flame, and subsequently nucleate or condense at lower temperatures downstream. These metals will form a suspended aerosol along with particles which are generated by other mechanisms. These are all convected along with the exhaust gases and can undergo various physical transformations which further influence the particle size distribution. An equation of convective diffusion can be derived. This equation represents a particle material balance over a volume fixed in space and can be written as:

$$\frac{\partial n}{\partial t} + \nabla \cdot nv = \nabla \cdot D\nabla n - \nabla \cdot nc + R_v \quad \mathrm{m^{-3}\,sec^{-1}} \quad (3)$$

where $n(v,x,t)$ ($\mathrm{m^{-3}}$) is the number size distribution, and where $n(v,x,t)\,dv$ is the number of particles per unit volume ($\mathrm{m^{-3}}$) in the particle volume range, v to $v + dv$, at position, x, and time, t. Particle volume, v, is used, rather than particle diameter, d_p, since for many simple theories employed here, total particle volume is a conserved quantity. The gas velocity is given by v ($\mathrm{m\,sec^{-1}}$), D is the Fickian particle diffusion coefficient ($\mathrm{m^2\,sec^{-1}}$), and c is the particle migration velocity resulting from external forces including gravity ($\mathrm{m\,sec^{-1}}$). $R_v(n,x,t)$ represents the net source of particles of size v, at position x, and time t, and includes several other internal physical processes which generate those particles. These internal processes include:

coagulation, which leads to particle growth due to particle adhesion or agglomeration, thus changing the psd, while conserving the total volume (or mass) of particles;

condensation, which changes the psd because of particle growth caused by mass transfer from the gas phase to an existing condensed phase; and

nucleation, which allows the formation of new particles directly from the gas phase.

Thus:

$$R_v = R_{\mathrm{coag.}} + R_{\mathrm{cond.}} + R_{\mathrm{nucl.}} \quad \mathrm{m^{-3}\,sec^{-1}}. \quad (4)$$

Other possible mechanisms include those in opposition to coagulation and condensation (fragmentation and evaporation), and sources other than nucleation (entrainment). Possible aerosol sinks include settling, inertial impaction, rainout, washout, diffusion to surfaces, and thermophoresis. Equation (3) is the continuous general dynamic equation (GDE) which describes the spatial and temporal evolution of a particle size distribution function, $n(v,x,t)$, including convective and diffusive terms. We are left to develop appropriate terms that account for the individual mechanisms and determine a solution or approximation to the GDE using appropriate initial and boundary conditions. Further discussion of coagulation, condensation, and nucleation processes follows.

6.1. *Coagulation*

6.1.1. *Mechanisms*

While coagulation (and fragmentation) processes modify the number density and size distribution of an aerosol, they cause no change in the total aerosol

mass (or volume) concentration. Formulation of the correct form for $R_{coag.}$ in the (continuous) GDE, can be achieved by first considering a discrete formulation for tracking particle collisions and growth by coagulation as functions of time and particle size as follows: Particles of size (volume) k are formed through collision of particles of size (volume) $k-i$ and size (volume) i (assuming that all collisions result in coagulation). They are also formed through the fragmentation of particles of size $k+i$ into particles of sizes k and i. Particles of size k are lost through their collision with any other particle or by fragmentation into particles of sizes i and j. For present purposes, we shall neglect fragmentation of the submicron and small supermicron particles Let $N_{i,j}$ be the number (frequency) of collisions per unit volume and time between particles of sizes i and j, given by:

$$N_{i,j} = \beta_{i,j} n_i n_j \qquad \mathrm{m^{-3}\ sec^{-1}} \quad (5)$$

where n_i and n_j are the number concentrations of particles of sizes i and j, respectively ($\mathrm{m^{-3}}$), and $\beta_{i,j}$ is the collision frequency ($\mathrm{m^3\ sec^{-1}}$), expressions for which are given later. Keeping track of the number of particles in each bin size, k, the rate of formation per unit volume of particles (size k) by coagulation can be shown to be:

$$\frac{dn_k}{dt} = \frac{1}{2}\sum_{i=1}^{k-i} \beta_{i,k-i} n_i n_{k-i} - \sum_{i=1}^{m} \beta_{i,k} n_i n_k \quad \mathrm{m^{-3}\ sec^{-1}} \quad (6)$$

where m is the maximum particle size in the distribution (∞). The factor 1/2 is included in Eq. (6) because collisions are counted twice in this summation. Equation (6) is the discrete coagulation equation for particles of size k. We extend this development to the continuous distribution function, $n(v,x,t)$ by defining $\beta(v,v')$ as the collision frequency between particles of sizes v and v', and converting the discrete summations to continuous integrals, thus:

$$R_{coag.} = \frac{1}{2}\int_0^v \beta(v',v-v')\, n(v',x,t)\, n(v-v',x,t)\, dv' - \int_0^\infty \beta(v',v)\, n(v,x,t)\, n(v',x,t)\, dv' \qquad \mathrm{m^{-3}\ sec^{-1}} \quad (7)$$

Equation (7) represents the source term describing coagulation for the continuous distribution function in the GDE (Eq. (3)). When the time rate of change of $n(v,x,t)$ is set equal to $R_{coag.}$, solutions to the resulting ODE represent either the time dependent change in the aerosol size distribution (due to coagulation) in a control volume, in the absence of convection or wall deposition or other internal processes, or alternatively, they represent the Lagrangian time dependent evolution of an aerosol, through coagulation only, in a parcel of fluid, traveling in steady 'plug flow' through a duct.

In combustion flue gases, the gas molecular mean free path is of the order of 0.1 μm. This turns out to be of the same size order as the evolving aerosol. Therefore, in developing appropriate expressions for the collision constant, one must consider transport phenomena in the free molecular regime ($Kn = 2l_g/d_p \gg 1$), in the continuum regime ($Kn \ll 1$), and in the transition regime between the two ($Kn \approx 1$), where l_g is the gas mean free path. Development of different forms of the collision frequency function are given by Friedlander.[162] For example, particles smaller than approximately 2 μm (diameter) collide as a result of Brownian motion. For spherical particles much larger than the gas mean free path ($Kn \ll 1$), particle collision is Brownian diffusion limited, and $\beta(v,v')$ takes the form:[163]

$$\beta(v,v') = 4\pi(D+D')\left(\frac{d_p + d_p'}{2}\right) \qquad \mathrm{m^3\ sec^{-1}} \quad (8)$$

where D and D', and d_p and d_p', are the diffusion coefficients and diameters, respectively, of the two particles of interest. Using a Stokes–Einstein formulation for D and D' yields:

$$\beta(v,v') = \frac{2kT}{3\mu}\left(\frac{1}{v^{1/3}} + \frac{1}{v'^{1/3}}\right)(v^{1/3} + v'^{1/3}) \qquad Kn \ll 1 \qquad \mathrm{m^3\ sec^{-1}} \quad (9)$$

for the continuum regime where k, T, and μ are the Boltzmann constant, temperature, and vicosity of the gas, respectively. Typically, the particle Brownian motion diffusion coefficient is much smaller than that for gas diffusion. The function $\beta(v,v')$ is a minimum when $v = v'$ and increases for coagulation of particles of unlike size.[164] For particles much smaller than the gas mean free path ($Kn \gg 1$), particle collision is described by the kinetic theory of gases and molecular collision:

$$\beta(v,v') = \left(\frac{3}{4\pi}\right)^{1/6}\left(\frac{6kT}{\rho_p}\right)^{1/2}\left(\frac{1}{v} + \frac{1}{v'}\right)^{1/2}(v^{1/3} + v^{1/3})^2 \qquad Kn \gg 1 \qquad \mathrm{m^3\ sec^{-1}} \quad (10)$$

where ρ_p is the particle density ($\mathrm{kg\ m^{-3}}$). For transition ($Kn \approx 1$) between the free molecular and continuum regimes, Fuchs[164] proposes an interpolation formula for $\beta(v,v')$ which is not given here. Note how the coagulation constants for both the continuum (Eq. (9)) and free molecular (Eq. (10)) regimes depend approximately on the square root of the combustion gas temperature (i.e. weakly).

Certain coagulation problems can be solved using a similarity transformation for the size distribution function.[165,166] As explained by Friedlander,[162] this similarity transformation is based on the assumption that the fraction of the particles in a given size range is a function only of particle volume normalized by the average particle volume. Therefore, the time taken to reach the 'self preserving' form depends on the shape of the initial distribution. 'Self preserving' means that the shape of the particle size distribution

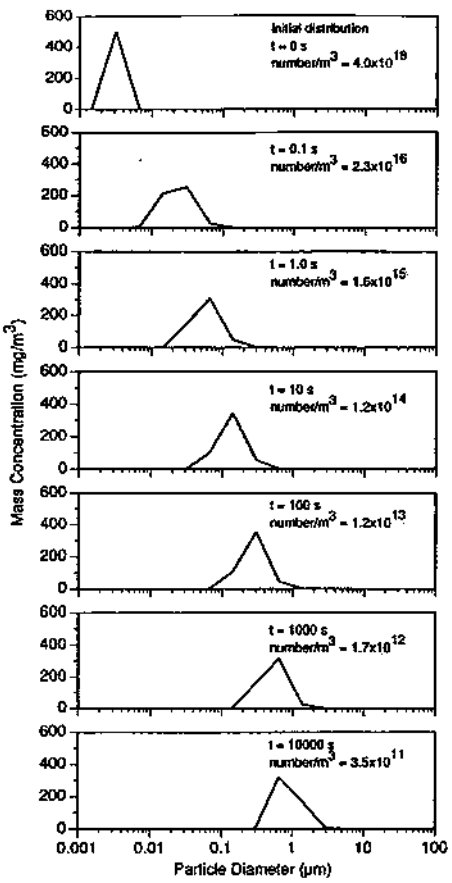

FIG. 13. Predicted evolution of lead oxide nuclei particles via coagulation in a post-flame combustion environment.

(psd) no longer changes, although the psd may move laterally along the particle size axis. The similarity transformation can be made for all coagulation mechansims in which the collision frequency is a homogeneous function of particle volume (i.e. for both continuum and free molecular regimes). The practical advantage of self preserving psd theory is that it allows *analytical* evaluation of the total number of particles, their average size, and the psd, as a function of time, if corresponding data at any one time are available.

When two molten metal particles coagulate, they will coalesce to form a single sphere of larger diameter. The surface area per unit mass will decrease. When two solid spherical particles agglomerate, but do not lose their initial shapes, the total surface area per unit mass does not change. Koch and Friedlander[167] developed a theory to account for the differences in coagulation behavior observed when combustion aerosols underwent a transition from viscous molten to solid states. The agglomeration process for non-molten solids was further analyzed by Matsoukas and Friedlander[168] who extended the self preserving psd theory to account for differing fractal properties of the agglomerated structures formed. They derived the important result that the average 'size' of the agglomerate, d_p, is given by:

$$d_p \sim d_{po}{}^{y}(\zeta,t) \qquad \text{m} \quad (11)$$

where d_{po} is the primary particle size, ζ is the volume of aerosol material, and $y < 0$ for agglomerates with a fractal dimension less than 3. As a practical matter, this means that, for a given particle concentration and time, the size of long chain-like particles (which have fractal dimensions less than 3) will *increase* as the size of the primary particles *decreases*; this result becomes more pronounced for agglomeration processes in the free molecular regime. This has implications in the formation of chain-like agglomerates from initially tiny nuclei, and suggests that these agglomerates can approach sizes of 1 μm diameter. Sizes larger than 1 μm have not been observed as a result of this process.

While Brownian motion has been widely studied and is the most appropriate mechanism to describe the collision and coagulation of small particles of interest in a combustion environment ($d_p < 2$ μm), other collision mechanisms including turbulent shear and differential sedimentation are possible and become important for larger particles. Friedlander[162] and Levich[169] discuss these mechanisms and present functional forms for their collision frequencies.

6.1.2. *Predictions*

Gelbard and Seinfeld[170] developed a multicomponent aerosol simulation code (MAEROS) to describe particle dynamics. This model can be applied to various environments including an aerosol evolving within a combustion or incineration system. The MAEROS code, and the previous single component version AEROSOL,[171–174] simulate the dynamics of a spatially homogeneous aerosol. The algorithms solve the GDE and can include terms to describe: coagulation due to Brownian motion, gravity, and turbulence; particle deposition due to gravitational settling, diffusion, and thermophoresis; particle growth due to condensation of a gas; and time varying sources of particles of different sizes and chemical compositions. MAEROS is intended as a general tool to supply necessary algorithms to solve the GDE for aerosol and other particulate systems. It is up to the user to configure the algorithms as necessary to apply to a particular environment of interest.

Figure 13 illustrates the predicted evolution of an aerosol due to coagulation only. The MAEROS code was used in which the particle size domain (d_p = 0.001 to 20.0 μm) was divided into 13 geometrically equal sections or bins. Coagulation was the only mechanism considered; all other mechanisms (condensation, nucleation, deposition, etc.) were disabled. At time zero, an initial mass of 500 mg m^{-3} was assigned to section 2 (d_p = 0.0021–0.0046 μm) to simulate the nucleation of a submicron fume. This aerosol was

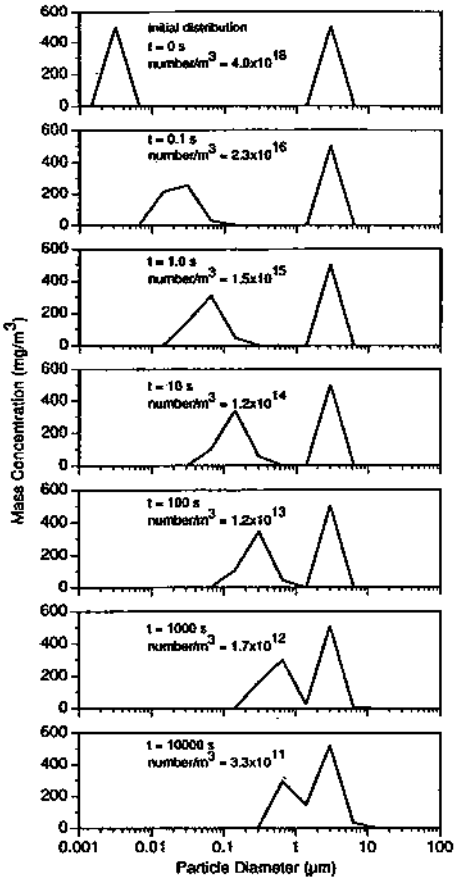

FIG. 14. Predicted evolution of lead oxide nuclei particles in the presence of a simulated sorbent via coagulation in a post-flame combustion environment.

assumed to have the properties of lead oxide, producing a number concentration of 4.0×10^{18} m^{-3}. Based on experience with coal combustion aerosols, and current RCRA particulate regulations of 180 mg m^{-3} after control, these initial conditions were deemed appropriate to model aerosol evolution through a hazardous waste incinerator. System pressure and temperature were maintained at 1.01×10^5 Pa (1 atm.) and 810 K (1000°F) to simulate post-flame conditions. The code does allow for changes in both pressure and temperature with time; however, this added complication was not deemed important because the dependence of β on temperature is only $T^{1/2}$. This effect is small compared to the number concentrations used in Eq. (7), and further, a constant (high) temperature only tends to increase coagulation rates compared to those seen using a decreasing temperature profile. Following the initial distribution, Fig. 13 presents six mass distributions which follow the evolving aerosol through six orders in time (t = 0.1, 1.0, 10, 100, 1000, 10,000 sec). Note that coagulation does not change the total aerosol mass and that the areas under all seven curves represent 500 mg m^{-3}. Number concentrations, however, are affected, and Fig. 13 shows that at 0.1 sec the number concentration has fallen approximately 2 orders of magnitude (2.3×10^{16} m^{-3}), and the average particle size has grown to approximately 0.03 μm. At 1.0 and 10.0 sec the distributions have grown only slightly farther into the d_p = 0.01–1.0 μm range. This is important, as these times represent a range of typical residence times within combustion/incineration systems. In fact, even after 10,000 sec (2.8 h) the average particle diameter is only approximately 1.0 μm with a number concentration of 3.5×10^{11} m^{-3}. Thus, as can be seen from Fig. 13, aerosol nuclei tend to coagulate very quickly at small times, due to the dependence on two rather large number concentrations (Eq. (7)), and then, at larger times, as number concentrations fall, coagulation slows considerably causing the aerosol to accumulate into a mode approximately between d_p = 0.1 and 1.0 μm. As discussed previously, particles in this size range exhibit minimum collection efficiencies in most APCDs. This characteristic distribution of a coagulating aerosol has been termed the accumulation mode. Note that the coagulation mechanism does not include the effect of differing fractal properties of the agglomerate formed, as developed by Matsoukas and Friedlander.[168] It has been assumed here that only spheres result from the coagulation process.

Figure 14 presents a second set of model calculations which predict the evolution of the same fume aerosol as in Fig. 13 but now in the presence of an aerosol of a larger size. These calculations are intended to simulate coagulation between an aerosol nuclei (toxic metal) and a sorbent which might be introduced in an attempt to remove particles from the accumulation mode where they are most difficult to collect. This simulation was conducted under the same conditions as those described previously with the addition of 500 mg m^{-3} of mass into section 11 (d_p = 2.0–4.4 μm) (total mass = 1000 mg m^{-3}). Evident from Fig. 14 is that coagulation between the evolving nuclei and the sorbent is very slow, and the small particles grow as if the sorbent were not present. Again, this is due in part to the large differences in number concentrations. At time zero, nuclei are present in concentrations of approximately 4.0×10^{18} m^{-3}. Sorbent particles are present in concentrations of 4.7×10^9 m^{-3}. This difference encourages nuclei–nuclei coagulation even though $\beta(v,v')$ is a minimum when $v = v'$ (Eq. (9)). Thus, it would seem that the use of a sorbent to scavange submicron toxic metal particles through coagulation is not possible in the times available. However, as has been described in previous sections, mechanisms other than coagulation may allow sorbents to be utilized to remove aerosol mass from the submicron fraction. Again, these results assume a fractal dimension of 3 (i.e. spheres) for the resulting agglomerates. Even though the simulation presented in Fig. 14 shows very little nuclei/sorbent interaction, fine particle coagulation and diffusion to the coarse mode are competitive processes. Friedlander *et al.*[175] reasoned that,

since diffusion and coagulation are first and second order with respect to particle number concentration, respectively, one should expect the following qualitative behavior. If, as presented in Fig. 14, particle nucleation results in a large initial number concentration, then coagulation will dominate, causing the nuclei to grow into particles with low diffusivities and little possibility to be scavenged by the coarse mode particles. If, on the other hand, nucleation results in a small initial nuclei number concentration, nuclei/nuclei coagulation rates will be small, the nuclei mode will not grow substantially but, provided sufficient residence time is available, will diffuse to, and be scavenged by, the coarse mode particles. Thus, using the self preserving size distribution theory, Friedlander *et al.*[175] argue that significant scavenging of nuclei by coarse mode (sorbent) particles is possible *if* the diffusion time (see Refs 17 and 175) is small compared to the residence time; and the mass of the fine mode is below a threshold value for a given coarse mode aerosol.

6.1.3. *Experimental results: coagulation mechanisms*

Matsoukas and Friedlander[168] have investigated the dynamics of the formation of metal oxide agglomerates from magnesium and zinc salts that were introduced into a flat flame. They also developed a theory for the agglomeration of fractal-like particles (chain-like and non-spherical particles) in the free molecular regime. Characteristic dimensions of the agglomerates followed a self preserving size distribution and, in agreement with theory, increased as the size of the primary nuclei particles decreased. Experimentally, the MgO agglomerates were more than twice as large as the ZnO agglomerates, where the ZnO agglomerates were composed of primary nuclei particles that were two to four times larger than those forming the MgO agglomerates. These authors also showed that the size distributions were wider than those for coalescing spheres.

The aerosol dynamics of lead oxide (PbO) particles formed in a bench scale flame reactor have been investigated by Biswas and co-workers at the University of Cincinnati.[176-179] Sethi and Biswas[176,177] focused on the competition between condensation and coagulation as the dominant growth mechanism when either lead acetate or silicon tetrachloride was introduced into a bench scale flame incinerator. They concluded that the dominant growth mechanism for the lead aerosol was condensation around existing (lead) nuclei, while that for the silicon aerosol was coagulation. Subsequent work on the lead/lead oxide aerosol from a bench scale flame[178] suggested that key parameters governing the evolution of the aerosol size distribution were the temperature history of the system, chemical reaction rates (lead to lead oxide), and the surface tensions of the various species. The idea that combustion conditions influence the resulting metal aerosol is further corroborated by the theoretical predictions of McNallan *et al.*[180] and by the experimental data of Scotto *et al.*,[44] which are discussed further in Section 6.3.

6.2. *Condensation*

6.2.1. *Mechanisms*

When supersaturation pressure of gaseous species are relatively low and large numbers of existing particles offer sufficient surface area, particle growth through heterogeneous condensation may occur. Heterogeneous condensation does not affect the aerosol number concentration, but allows for mass (or volume) addition through growth of existing particles. Heterogeneous condensation of a species onto the surface of an existing aerosol can be described by the combination of a source term or growth law, $I(v)$, which describes the size dependent driving force for mass addition through condensation for particles of size v (including chemical and physical properties of the system) times the number density of particles of size v, $n(v,x,t)$, at position x, and time t:

$$R_{\text{cond.}} = \frac{\partial}{\partial v}[I(v)n(v,x,t)] \qquad \text{m}^{-3}\,\text{sec}^{-1} \quad (12)$$

where $I(v) = \mathrm{d}v/\mathrm{d}t$ has units of $\text{m}^{-3}\,\text{sec}^{-1}$. Growth laws for diffusion, molecular bombardment, surface reaction, and droplet phase reaction are given by Friedlander.[162] For example, as with coagulation, in the continuum regime ($Kn \ll 1$) growth is limited by the rate of transport of a condensing species to the particle surface. The rate of diffusional condensation of a species i on a single particle of (constant) size, d_p for the continuum range, is derived from Fick's Law in a quiescent medium as:

$$F_i(d_p) = \frac{2\pi d_p D_{im}}{RT}(P_i^{\infty} - P_i^{sat}) \qquad Kn \ll 1 \qquad \text{gmol sec}^{-1} \quad (13)$$

where D_{im} is the pseudo binary diffusion coefficient, R is the gas constant, and P_i^{∞} and P_i^{sat} are the condensing species vapor pressures far from and near the particle surface, respectively. Depending on the particle size and the nature of the condensing species, P_i^{sat} may be influenced by the Kelvin Effect which results in an increase in the equilibrium vapor pressure inside capillaries and over curved compared to flat (exterior) surfaces, and the Solute Effect, whereby mixtures in solution tend to lower the individual equilibrium vapor pressures compared to pure species. Multiplying Eq. (13) by the gram-molar volume of the condensed species (M_{wi}/ρ_i) yields the growth law with appropriate units as:

$$I(v) = \frac{\mathrm{d}v}{\mathrm{d}t} = \frac{2\pi d_p M_{wi} D_{im}}{\rho_i RT}(P_i^{\infty} - P_i^{sat}) \qquad Kn \ll 1 \qquad \text{m}^3\,\text{sec}^{-1} \quad (14)$$

where M_{wi} and ρ_i are the condensing species molecular weight (kg gmol^{-1}) and density (kg m^{-3}), respectively. For particles much smaller than the gas mean free path, the rate of condensation is given by molecular interactions and kinetic theory:

$$F(d_p) = \frac{\varphi \pi d_p^2}{(2\pi M_{wi} RT)^{1/2}} (P_i^\infty - P_i^{sat})$$

$$Kn \gg 1 \qquad \text{gmol sec}^{-1} \quad (15)$$

and:

$$I(v) = \frac{dv}{dt} = \frac{\varphi \pi d_p^2 M_{wi}}{\rho_i (2\pi M_{wi} RT)^{1/2}} (P_i^\infty - P_i^{sat})$$

$$Kn \gg 1 \qquad \text{m}^3 \text{ sec}^{-1} \quad (16)$$

where φ is an accommodation coefficient which is determined experimentally (or assumed to be unity). In the development of these growth laws, several assumptions were made including: ideal condensing gas, negligible temperature effects due to latent heats of condensation, particle and condensing species have similar densities, and negligible diameter changes due to condensation (thin film approximation). As with coagulation, an interpolation formula has been developed to approximate the rate of condensation over the transition range ($Kn \approx 1$).[181]

The mass fraction of a condensed species, $W_i(d_p)$, is given by the mass condensed (in time, t) on a particle of size d_p, divided by the particle mass:

$$W_i(d_p) = \frac{M_{wi} \int_0^t F(d_p) dt}{\frac{\pi}{6} \rho_p d_p^3}. \quad (17)$$

Different condensation mechanisms will yield different dependencies of $F(d_p)$ on d_p. In the cases that follow, it is assumed that d_p does not change appreciably with time (thin film approximation). Continuum film diffusion (Eq. (13)) yields $F(d_p) \sim d_p$, thus:

$$W_i(d_p) \sim 1/d_p^2 \qquad Kn \ll 1 \quad (18)$$

while free molecular film diffusion (Eq. (15)) yields $F(d_p) \sim d_p^2$, and thus:

$$W_i(d_p) \sim 1/d_p \qquad Kn \gg 1. \quad (19)$$

Species i may also react at the surface of a particle of diameter, d_p. The reaction rate at the surface per unit area, R_i is given by:

$$R_i = \frac{k_r}{RT} P_i^s \qquad \text{gmol m}^{-2} \text{ sec}^{-1} \quad (20)$$

where k_r(m sec^{-1}) is the surface reaction rate coefficient and P_i^s is the partial pressure of species i at the surface. Note that P_i^s may be much less than P_i^{sat} allowing this process to occur at temperatures higher than the dewpoint. Considering both continuum diffusion and surface reaction, the flow of species i to the surface is given by:

$$F_i(d_p) = \frac{\pi d_p^2}{RT} \left(\frac{1}{\frac{1}{k_r} + \frac{d_p}{2D_{im}}} \right) P_i^\infty \quad \text{gmol sec}^{-1} \quad (21)$$

which reduces to Eq. (13) for $k_r \gg 2D_{im}/d_p$ (diffusion controlled regime), and consequently, a $1/d_p^2$ dependence for $W_i(d_p)$. Under external surface *reaction controlled* conditions ($k_r \ll 2D_{im}/d_p$):

$$F_i(d_p) = \frac{k_r \pi d_p^2}{RT} P_i^\infty \qquad \text{gmol sec}^{-1} \quad (22)$$

leading to:

$$W_i(d_p) \sim 1/d_p \qquad \text{when:} \quad k_r \ll \frac{2D_{im}}{d_p}. \quad (23)$$

For the free molecular regime, Haynes *et al.*[72] showed that reaction controlled conditions occur when the probability, q, of reaction upon collision of a molecule of species i with the surface is much smaller than the Knudsen number. According to molecular collision theory (see Haynes *et al.*[72]):

$$k_r = \frac{qD_{im}}{2.6 l_g} \qquad \text{m sec}^{-1} \quad (24)$$

which shows that k_r does not depend on particle size.

The particle may be porous, in which case diffusion/reaction interactions inside the particle become important. The true internal surface area per unit mass, S (m^2 kg^{-1}), does not depend on d_p, and the flow of species i from the surface into the particle is given by:

$$F_i(d_p) = \frac{\pi d_p^3 \rho_p \varepsilon S k_r}{6RT} P_i^s \qquad \text{gmol sec}^{-1} \quad (25)$$

where ε is the effectiveness factor[182] and k_r (m s^{-1}) is the true intrinsic reaction rate coefficient. The effectiveness factor, ε, depends on the Thiele Modulus [$h_p = d_p/2(\rho_p S k_r/D_e)^{1/2}$] and, for $h_p > 3$ (i.e. pore diffusion controlled conditions), $\varepsilon = 1/h_p$ or:

$$\varepsilon = \frac{2}{d_p} \left(\frac{D_e}{\rho_p S k_r} \right)^{1/2} \ll 1 \quad (26)$$

and $P_i^s = P_i^\infty$ if film diffusion is neglected. D_e is the effective diffusivity (m^2 sec^{-1}) within the particle, and depends on molecular and Knudsen diffusivities as well as porosity. Inspection clearly shows that under pore diffusion controlled conditions:

$$W_i(d_p) = \frac{M_{wi} \int_0^t \frac{\pi d_p^3 \rho_p \varepsilon S k_r}{6RT} P_i^s dt}{\frac{\pi}{6} \rho_p d_p^3} \sim \frac{1}{d_p}$$

$$\text{when: } h_p > 3 \quad (27)$$

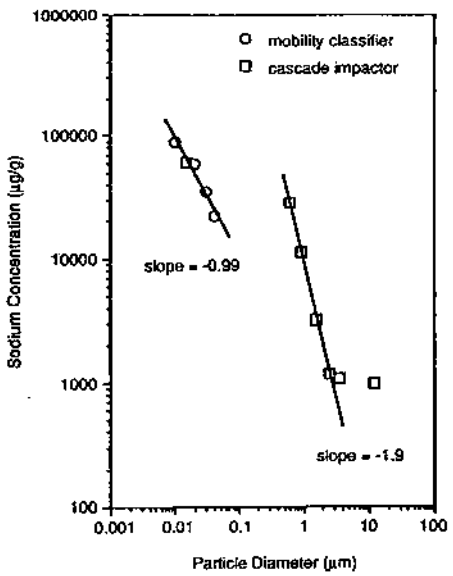

FIG. 15. Film condensation of sodium on coal ash particles in the free molecular and continuum regimes showing $1/d_p$ and $1/d_p^2$ dependencies, respectively (adapted from Neville and Sarofim[151]).

which is similar to the external surface reaction controlled case. This is not surprising since pore diffusion control implies that reaction takes place close to the surface, but inside the particle.

In summary, a metal species which either condenses or reacts on or near the surface of a particle will demonstrate enrichment on small particles. Under a thin film approximation [$d_p \neq d_p(t)$], the overall metal concentration, W_i, on the particle will depend on d_p as:

$$W_i \sim \frac{1}{d_p^2} \tag{28}$$

either for condensation ($P_i^\infty > P_i^{sat}$) around particles whose diameters are much greater than the mean free path of the gas ($d_p \gg l_g$), or for conditions of continuum diffusion controlled surface reaction, where, P_i^∞ may be less than P_i^{sat}. Alternatively:

$$W_i \sim \frac{1}{d_p} \tag{29}$$

either for free molecular condensation ($P_i^\infty > P_i^{sat}$) around small particles whose diameters are smaller than the mean free path of the gas ($d_p \ll l_g$), or for external surface reaction controlled conditions, for all particle sizes, large and small, where P_i^∞ may be much less than P_i^{sat}; or for pore diffusion controlled reaction inside the particle, for all particle sizes where P_i^∞ may be less than P_i^{sat}. For reaction controlled conditions inside a very porous particle ($\varepsilon \approx 1$), there is no dependence of d_p on W_i (i.e. no enrichment).

6.2.2. *Experimental results: condensation and surface reaction mechanisms*

The theory presented above, suggests that different condensation mechanisms can lead to different dependencies of metal concentration with respect to particle size. In this section, we present experimental data on what metal condensations mechanisms are actually observed in combustion processes. Figure 15 depicts, for sodium in coal flyash, a $1/d_p$ dependence in the free molecular regime and a $1/d_p^2$ dependence in the continuum regime.[151] This suggests that film condensation is the mechanism controlling sodium enrichment in these particles. Gallagher *et al.*[40] found that the slope of the $1/d_p^2$ dependence in the continuum regime, decreased with increasing temperature. This phenomenon was attributed to sodium capture by silicon. Neither the larger particles ($d_p > 4\,\mu m$) nor the very small particles ($d_p < 0.4\,\mu m$) followed a $1/d_p^2$ dependence, probably because significant amounts of sodium were present in the bulk particles of both size extremes. Biermann and Ondov[67] suggested that for coal, a $1/d_p^2$ dependence for arsenic, selenium, and tungsten was superior to a $1/d_p$ dependence, over a particle size range from 0.1 through 10 μm, although both correlations coincided for $d_p > 0.8\,\mu m$. Davison *et al.*,[52] and Haynes *et al.*,[72] on the other hand, both strongly suggest that many toxic metals (arsenic, nickel, and cadmium in Davison's study and arsenic, antimony, potassium, manganese, vanadium, and tungsten in Haynes' study) followed a $1/d_p$ dependence rather than a $1/d_p^2$ dependence over particle sizes $0.4\,\mu m < d_p < 10\,\mu m$ (i.e. over the continuum range). Haynes, in fact, corroborated the $1/d_p^2$ dependence of other researchers for sodium, but found that to be the exception. The $1/d_p$ dependence for toxic metal enrichment under continuum conditions is very significant, since it suggests that many toxic metals may be reactively scavenged by existing flyash particles as opposed to merely being condensed on them. This may have a significant positive bearing on both the potential capture of trace quantities of toxic metals in the vapor phase and the potential water leachability of toxic metals in the collected ash. In conclusion, the data show that surface condensation can account for the sodium mass contribution to the mid particle size range, although very small particles may consist of a sodium fume, and large particles may contain sodium distributed throughout. Many metals on the other hand appear to be reactively scavenged or chemisorbed on existing particles, although the generality of this hypothesis remains to be established. This topic will be addressed again later.

6.3. *Nucleation*

Self-nucleation, or homogeneous condensation, changes both the aerosol number and mass (or

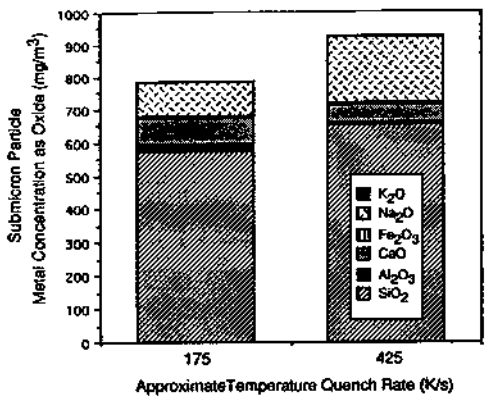

FIG. 16. Effect of temperature quench rate on submicron flyash particle composition from coal combustion (adapted from Scotto *et al.*[44]).

volume) concentrations, through the formation of new particles from gas-phase precursors. In general, heterogeneous condensation onto the surfaces of existing particles is thermodynamically favored over homogeneous nucleation. McMurry and Friedlander,[183] while examining new particle formation in the presence of an existing aerosol, concluded that the effect of increasing the initial aerosol number concentration was to suppress new particle formation. However, when sufficient sites for condensation do not exist or when supersaturation pressures are sufficiently high, self-nucleation may occur. Nucleation rate theories[184] attempt to describe the formation of molecular clusters, each very small and containing only a few molecules. Details of the nucleation theory can be found in Friedlander.[162] If we consider a stable unsaturated vapor, attractive forces between individual molecules force the formation of molecular clusters. At equilibrium, a balance exists between the addition and removal of vapor molecules from a cluster of size d_p and one can define a critical nucleus size d_p^* as:

$$d_p^* = \left(\frac{4\sigma v_{mi}}{kT \ln S_i}\right) \qquad \text{m} \quad (30)$$

or:

$$d_p^* = \frac{4\sigma M_{wi}}{\rho_i RT \ln S_i} \qquad \text{m} \quad (31)$$

where $S_i = P_i/P_i^{sat}$ is the supersaturation ratio, σ is the surface tension, and v_{mi} and ρ_i are the molecular volume and density of the liquid, respectively. Clusters smaller than d_p^* tend to evaporate, while clusters larger than d_p^* tend to grow.

Let n_g represent the number of clusters containing g molecules. The droplet current, I_g, is defined as the difference in the rate, or excess rate, at which clusters pass from size $g - 1$ to g (condensation) compared to g to $g - 1$ (evaporation). Under the assumptions of rapid equilibrium between small cluster sizes, absence of large clusters, and a quasi-steady state existing such that droplet current (I) is independent of particle size ($\partial n_g/\partial t = -\partial I/\partial g \approx 0$), the droplet current, or the rate of generation of nuclei particles, can be expressed as:

$$I = A \exp\left(\frac{-B}{(\ln S_i)^2}\right) \qquad \text{m}^{-3}\,\text{sec}^{-1} \quad (32)$$

where A and B depend on temperature, surface tension, droplet mass, monomer partial pressure, and liquid density. S_i, the supersaturation ratio (P_i/P_i^{sat}), is a very strong function of temperature, and the droplet current is extremely sensitive to that quantity. As a result:

$$R_{nucl.} = I = A \exp\left(\frac{-B}{(\ln S_i)^2}\right) \quad \text{when:} \quad d_p = d_p^* \qquad \text{m}^{-3}\,\text{sec}^{-1} \quad (33)$$

and:

$$R_{nucl.} = 0 \qquad \text{when:} \quad d_p \neq d_p^* \quad \text{m}^{-3}\,\text{sec}^{-1} \quad (34)$$

The above expressions suggest that the competition between *homogeneous nucleation*, with a very nonlinear dependence on P_i^{sat}, and *heterogeneous condensation*, with a linear dependence on P_i^{sat}, can be adjusted by varying the temperature quench rates (dT/dt) in a combustor. Nucleation and condensation of metal vapors in the neighborhood of burning coal particles has been investigated theoretically by Senior and Flagan[185] and Helble *et al.*[186] The effect of dT/dt has been theoretically investigated by McNallan *et al.*,[180] who suggested that homogeneous nucleation of fine silica may occur at temperatures above 1700 K in spite of the presence, in the gases, of preexisting particles, when the gases are cooled at a rate in excess of 600 K sec^{-1}. The experimental data[44] shown in Fig. 16 further support the hypothesis that increased temperature quench rate increases the emission of small nuclei, although these data suggest that the increase was limited to that of sodium fume. This result is in agreement with the results of Taylor and Flagan[187] and Lin *et al.*,[178] in that it suggests that combustion conditions, including temperature quench rate, can have a large influence on the nature of the size-segregated metal aerosol produced.

7. TOXIC METAL CAPTURE BY SORBENTS

7.1. *Introduction*

We have seen that the mechanisms governing the fate of toxic metals during combustion/incineration may be determined in part long before the fuel or waste is fed into the combustor. Other mechanisms depend on the combustion environment and the presence of other species. Aerosol formation processes commence when the toxic metal is mobilized into the vapor form (a process which is enhanced by the presence of chlorine). As temperatures decline, the

supersaturated metal will be forced from the vapor phase, either by nucleation to form new particles, or by mass transfer with or without surface reaction, to enrich the composition of existing particles. The general dynamic equation may be used to describe the formation and evolution of the particle size distribution (containing toxic metals) with time. We have noted that coagulation alone is insufficient to cause the submicron toxic metal aerosol to grow into the supermicron range, especially within residence times available during post-combustion processes. Furthermore, the availability of large surface areas offered by existing submicron particles will promote simple condensation and toxic metal enrichment on these small respirable particles. With respect to the ultimate emissions and subsequent health risks, determination of the toxic metal speciation is at least as critical as determination of the particle size distribution since multimedia aspects of the toxic metals problem demand that these toxic metals be isolated from the environment in such a way that they are neither inhaled nor ingested and that they form water unleachable compounds. One mechanism through which this may be achieved is to react, not merely condense, the metal on the surface of reactive sorbents to form glass-like compounds containing (and isolating) the toxic metal in question. The critical questions include: are such sorbents available and economical, can they be exploited at the hostile post-flame environment prior to metal nucleation/condensation, and if glass-like eutectic products are formed, does the process occur rapidly enough to capture sufficient quantities of the metal before the kinetics are slowed, new nuclei are formed, or the pores are closed due to high temperature sorbent sintering? This section addresses these questions and attempts to show how metal emissions from incinerators may be controlled by reaction with simple sorbents.

7.2. *Capture of Lead and Cadmium in a Bench Scale Thermogravimetric Reactor*

Uberoi and Shadman[188,189] conducted a series of experiments in which various sorbents could be screened to determine their potential for the capture of lead and cadmium. The apparatus used was a thermogravimetric reactor described in detail by Uberoi.[190] The metal compound (chloride) was suspended by a platinum wire from a microbalance, which monitored the weight change during the experiments. Individual packed microbeds of 100 mg of sorbent particles placed on a 100 mesh stainless steel screen in a quartz insert were constructed out of several commercial sorbents (silica, alumina, kaolinite, bauxite, Emathalite, and limestone) with compositions shown in Table 10. The temperature of the sorbent bed was higher than the temperature at which the metal source was vaporized (approximately 700°C vs 495°C for lead and 800°C vs 560°C for cadmium), thus ensuring that phenomena other than simple surface condensation, were investigated. The metal vapor was transported through the sorbent bed by a simulated flue gas (15% CO_2, 3% O_2, 80% N_2, and 2% H_2O) and the metal uptake in the sorbent bed (measured by atomic absorption) was compared to the metal delivered (microbalance), with the results shown in Figs 17a and b. Water soluble metal represents that fraction that could be extracted by water at 40°C in an ultrasonic bath for 2 hr, and the remainder is denoted as water insoluble. Note that the lead and cadmium results are significantly different. While several simple sorbents are effective for lead removal (silica, alumina, kaolinite, bauxite, and Emathlite), fewer are effective for cadmium removal (alumina and bauxite). One might identify the water insoluble fraction as that fraction that is chemisorbed or reactively adsorbed, while the water soluble fraction is that which is merely physisorbed. Limestone was not effective at reactively capturing either metal. That kaolinite is very effective for lead but not at all effective for cadmium may be attributable to pore plugging for cadmium. X-ray diffraction analyses revealed the crystalline structure of both monoclinic and hexagonal $PbAl_2SI_2O_8$ for lead, suggesting the following overall reaction for that compound:

$$Al_2O_3 \cdot 2SiO_2 + PbCl_2 + H_2O \longrightarrow PbO \cdot Al_2O_2 \cdot 2SiO_2 + 2HCl. \quad (35)$$

Clearly, this is a process of reactive adsorption, and the presence of water vapor as a reactant is required. At this point the appropriate kinetics still remain to be determined, and this idea of reactive scavenging must still be optimized to be put into practice.

7.3. In Situ *Capture of Lead in a Laboratory Combustor*

One approach to exploit the bench scale results of Uberoi *et al.*[191] and Uberoi and Shadman[188,189] is to inject sorbent into a flow combustor in an attempt to effect the *in situ* reactive capture of toxic metals in that environment. This technique has been investigated by Scotto *et al.*,[148] who conducted experiments on the capture of vaporized lead by kaolinite injection downstream of the primary flame in a 17 kW down-flow combustor. As described in Section 5, an aqueous lead acetate solution was injected through a natural gas flame at a stoichiometric ratio of approximately 1.2 to produce approximately 100 ppm of lead vapor in the exhaust. Particle size distributions were measured both with and without sorbent injection and, in addition to particle measurement using a DMPS, particles were also sampled using a 30 lpm Andersen impactor. The effect of chlorine, added to the combustion air at chlorine/lead molar ratios of 2 and 10, was also examined.

TABLE 10. Composition of various sorbents (adapted from Uberoi and Shadman[189])

Weight percent	Silica	Alumina	Kaolinite	Bauxite	Emathlite	Limestone
SiO_2	100.0		52.1	11.0	73.4	0.7
Al_2O_3		100.0	44.9	84.2	13.9	0.3
Fe_2O_3			0.8	4.8	3.4	0.3
TiO_2			2.2		0.4	
CaO					5.0	97.2
MgO					2.6	1.5
K_2O					1.2	
Na_2O					0.1	

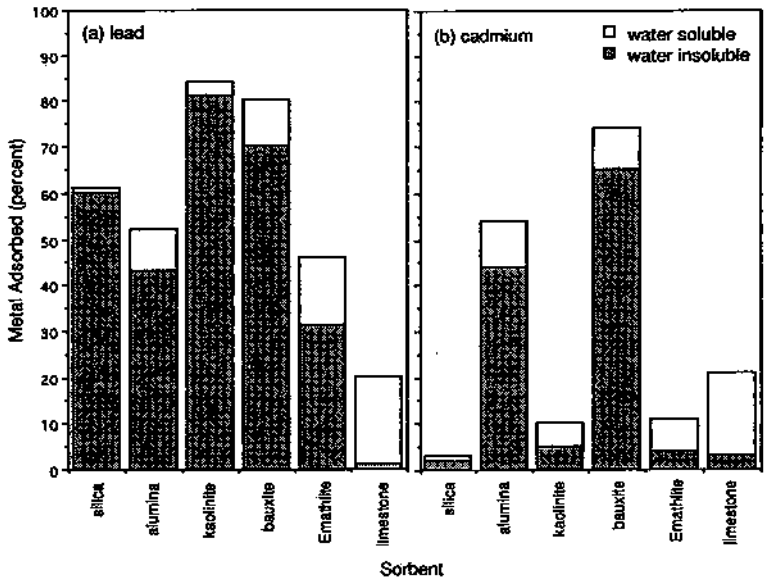

FIG. 17. Thermogravimetric reactor: capture of (a) lead and (b) cadmium by sorbents (adapted from Uberoi and Shadman[188,189]).

Results presented in Fig. 18 show that, in the absence of chlorine, addition of a kaolinite sorbent was extremely effective in scavenging the lead vapor which, in the absence of the kaolinite sorbent, produced a submicron aerosol via nucleation.[148] In fact, Fig. 18 shows an approximate 99% reduction in the submicron ($< 0.5\,\mu m$) particle number and volume distributions. The kaolinite had an approximate mass mean size of $2.0\,\mu m$ diameter. Impactor samples showed that the ratio of lead/aluminium was independent of particle size (averaging 0.971), with no lead enrichment on the smaller particles. This suggests an internal surface reactive capture mechanism under reaction controlled conditions (with an effectiveness factor equal to unity). This is in sharp contrast with coal ash data[72] where enrichment on smaller particles follows either a $1/d_p$ dependence, when reaction at or near the external surface controls, or a $1/d_p^2$ dependence when film condensation controls (see Section 6.2). The average lead/aluminum ratio of 0.971 was consistent with electron diffraction X-ray (EDX) analyses of individual particles and corresponds to a sorbent utilization rate of 25% if the reaction product is the same as that proposed by Uberoi and Shadman[188] (see Eq. (35)). Scanning electron micrograph (SEM) images showed that all sorbent particles that contained lead also melted, even though the melting point of pure kaolinite (2083°C) far exceeded any that was achieved during the experiment. It was concluded that the partial utilization of sorbent occurs because of reactive scavenging of the lead by the sorbent. Furthermore, as has been shown in Section 6.1, coagulation processes are incapable of achieving the observed reductions in concentration of submicron lead particles. Therefore, the process was one of reactive adsorption, not physical coagulation.

When chlorine (chlorine/lead molar ratio of 2) was added, the kaolinite sorbent was still very effective in reactively scavenging lead vapor. This stoichiometry is analogous to that investigated by Uberoi and Shadman[188] for lead. However, when a large excess of chlorine was added (chlorine/lead molar ratio of 10), the sorbent ceased to be effective under the conditions examined. The reasons for this have not been unambiguously determined, but one possible explanation might be that the most effective capture is that of the metal oxide. In the bench scale studies of Uberoi and Shadman, an equilibrium between the oxide and chloride allows significant amounts of the

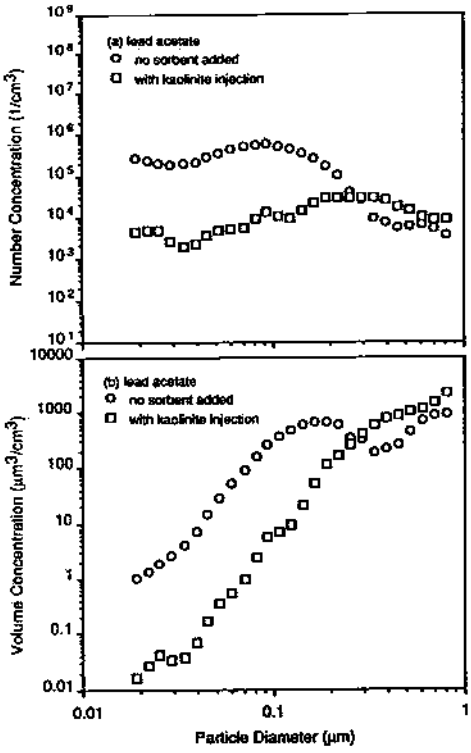

FIG. 18. Laboratory combustor: *in situ* capture of lead by kaolinite sorbent (adapted from Scotto *et al.*[148]).

oxide to be formed and immediately scavenged by the sorbent, thus causing a net removal. As more chlorine is added, the equilibrium shifts towards the chloride, which is less reactive. Future research could uncover these mechanisms more precisely.

7.4. *Capture of Toxic Metals in a Fluidized Bed Incinerator*

Ho *et al.*[192–194] have undertaken a far ranging study to investigate fluidized bed technology for metal emission control. Bed/sorbent materials consisting of silica (sand), alumina, and limestone were fluidized at specific temperatures, maintained with a preheater. Wood, impregnated with lead nitrate or lead chloride, was charged into the 76 mm diameter bed at a constant rate. It was found that lead capture by sand depended on bed temperature, with an optimum at approximately 700°C. At lower temperatures the metal failed to be released and was carried out with unburned carbon. At higher temperatures it was released rapidly and failed to be captured. Ho *et al.*[194] suggest the following mechanisms for metal capture in their fluidized bed: trapping of the metal by melted ash from the wood, and subsequent coalescence of the liquid with sorbent particles; vapor capture, similar to that investigated by Uberoi and Shadman[198] and Scotto *et al.*,[148] and particulate capture through coagulation of condensed metal aerosol with sorbent particles in the fluidized bed. According to Litt and Tewkesbury,[103] particulate capture by sorbents in fluidized beds will be enhanced if the sorbent surface becomes 'chemically or physically' sticky, and sodium compounds might be added to promote this. Possibly some modification of this idea might be applicable in entrained flow systems, where collapsing of the bed would be less of a problem. Sticky particles in fluidized beds can cause fluidization to cease and the pressure drop to increase uncontrollably. Future research could address this problem.

8. CONCLUSIONS

Toxic metal emissions into the environment are ubiquitous, and arise from a large number of different combustion processes, ranging from fossil fuel combustion to hazardous and municipal waste incineration, and industrial processes. Regulations limiting the airborne releases of toxic metals can be based either on a risk assessment analysis, as in the case of RCRA regulation in the U.S., or on simple emission limits, as is the case for the CAA regulation in the U.S. and the EC directives. Toxic metals can neither be manufactured nor destroyed in a combustion process, but they can be transformed both chemically and physically. In assessing the risks associated with toxic metals in combustion, one must address the whole multimedia problem. Toxic metals may exit the process in molten slag, in dry collected ash, in wet scrubbed ash, or as an airborne aerosol exiting the stack. In each case the metal may enter the environment and affect humans through groundwater contamination, through deposition on fields and subsequent uptake in the food chain, or through inhalation. The environmental impact of each of these processes can be greatly influenced by metal transformations occurring in the combustion chamber, and these are determined by both the composition of the inlet feed, and the combustion conditions themselves. In fact, it is desirable to use the high temperature conditions of the combustion process to manufacture benign forms of the metal that can be isolated from the environment.

Extensive literature exists on metal emissions from coal combustion. This essentially consists of size segregated particle compositions of flyash, and shows that many toxic metals are concentrated in the submicron particle size range. This particle size range is difficult to collect and remove from combustion flue gases. In comparison to the coal literature, that on metal emissions from various incineration and industrial processes is more sparse, and so we must use some of the coal results to gain insight into the fate of metals in these less conventional combustion processes.

Toxic metals may be introduced into the combustion chamber in a great variety of chemical and physical forms. Furthermore, there is a range of

combustion environments in which the metals are subsequently processed. Of interest is to determine the extent to which these variations affect the subsequent transformation of the metal before it leaves the process. The overriding questions are:

(1) Will the metal leave the combustor as submicron particles or vapors, which are difficult to collect and isolate from the air environment, or will it combine with easily collectable large ash particles, which may, either with or without further treatment, be isolated also from the aquatic or soil environment?

(2) How does the combustion process transform the speciation of the metal in question, and can the high temperature environment of the combustor be used to transform a potentially toxic metal species into an environmentally benign form?

Metals may be contained in solid or liquid fuels, chemically bound to the organic fuel matrix (inherent mineral matter), dispersed within the fuel particle as mineral crystallites (included mineral matter), or, indeed, completely separate from the fuel particle (excluded or extraneous mineral matter). Alternatively, toxic metals may enter as chemically bound organometallic compounds, as in paints, pigments, or chelated compounds. One might expect these to behave like organic mineral matter in fuels. Metals may enter together with other inorganic clays and soils, as during the thermal treatment of contaminated soils, or they may be contained in aqueous solutions and sludges. Toxic metals may be introduced continuously together with the combustible waste, or in batch drums, as in rotary kilns. They may be introduced into the combustion chamber as single salts or individual compounds, or they may enter as a mixture.

The key issues regarding mechanisms are:

(1) By what mechanisms and at what rates are volatile metals released into the hot gas phase inside the combustor, and how do these depend on combustion variables?

(2) What is the composition of the size segregated aerosol formed in the presence of a condensing toxic metal?

(3) How does the size distribution of the aerosol consisting of metal nuclei evolve with residence time, both in the absence and in the presence of much larger particles?

(4) Can toxic metal vapor be reactively scavenged by sorbents to form environmentally benign compounds?

Chlorine has a profound influence on the partitioning of many toxic metals between vapor and condensed phases in the combustor. Equilibrium predictions suggest that chlorine can strongly influence the relative split between hexavalent and trivalent chromium. Upon entry, the metal-containing waste may be transformed into various physical forms. Dissolved metal salts, such as metal nitrates or pyrites, for example, will form reactive metal compounds which may decompose violently at elevated temperatures. This process will occur after water or other solvents have evaporated, a process that can take some time if the droplets are large.

Upon cooling, the metal will nucleate homogeneously, or condense on existing particles, to form an evolving aerosol. This will occur at temperatures *below* the dewpoint (which depends on the overall composition), and the particle size distribution leaving the combustor will depend on how much time the metal aerosol was allocated after the dewpoint was reached. This aerosol will consist of small particles which are difficult to collect, and which are most likely to consist of toxic metal species. Even if heterogeneous condensation around existing particles dominates, this will also lead to strong enrichment of toxic metals on the small particles. This scavenging process can occur only at temperatures *below* the metal dewpoint, which may be below reasonable temperatures in the combustor. However, if the metal can be made to *react* with other ash aerosol (or sorbent) particles, the scavenging process occurs *above* the dewpoint, and since such a reaction may have a high activation energy, it can in fact, be enhanced by the high temperatures present in incinerators.

Alternatively, the metal compound may become embedded inside a porous char matrix. This will happen, for example, to organic metals in oil or both inherent and included mineral matter in pulverized coal. It may also occur for organo-metallic liquids, although this depends on the volatility of these liquids and whether they are more similar to light oils which vaporize rapidly without char formation or to heavy oils which form carbonaceous residues upon being heated. If a residual char is not formed it is reasonable to expect that the metal will behave similarly to metals in aqueous solutions (at the same temperature), where vaporization results either in a metal vapor or in residual metal particles, one per drop. If char, containing organically bound metal, is formed, the metal contained in the char must be released within the char matrix, subsequently to diffuse through it, or it will enter the gas phase as the char matrix itself is oxidized. In the former process, there is the opportunity for the metal to react with included silicates to form stable compounds that fail to vaporize. Alternatively, the metal which has been released may diffuse back into the char matrix remaining, to react with included silicates situated there or it may react with extraneous silicates. Finally, there is evidence that one metal (sodium), may displace another metal (potassium), which would otherwise be immobile, bound in a stable mineral form such as illite.

Aerosol dynamic processes governing the temporal size distribution of an airborne aerosol must be considered in any attempt to model the fate of metals

during combustion. Theoretical calculations which describe the temporal size evolution of an airborn aerosol have shown that, under incineration conditions, coagulation alone is insufficient to form collectable large particles from tiny nuclei resulting from homogeneous condensation. These calculations also show that coagulation cannot readily be used to scavenge tiny nuclei by large sorbent particles. Future work, however, could be to explore the potential of using non-uniform coagulation processes to form structures with fractal dimensions of less than 3.

It has been shown that many volatile metals can be reactively scavenged by commercial sorbents. It has also been shown that this scavenging process can be employed *in situ* in the combustor, for the case of lead being scavenged by kaolinite. This process is intriguing, since it suggests that the high temperatures in the combustor can be used for an environmentally friendly purpose to isolate toxic metals, rather than produce only environmentally hostile effects by enhancing metal vaporization. Future work could optimize this process and determine the pertinent mechanisms. Future work could also develop multifunctional sorbents that can react and scavenge more than one metal compound, and also possibly chlorine. When a metal is initially contained in contaminated soils, or in mixed sludges and slurries, it forms, upon introduction into a hot furnace environment, an inorganic mixture containing both the toxic metal and potential scavenging agents, such as clays and glasses. It is not surprising, therefore, that upon heating, much of the toxic metal will react with the clay and only a little will be released to form a condensable vapor. Again, the exact mechanisms have not been determined, although work is in progress on this subject.

Acknowledgements/Disclaimer—Portions of this work were conducted under EPA Purchase Order 1D2969NTTA with J. O. L. Wendt. The research described in this article has been reviewed by the Air and Energy Engineering Research Laboratory, U.S. Environmental Protection Agency, and approved for publication. The contents of this article should not be construed to represent Agency policy nor does mention of trade names or commercial products constitute endorsement or recommendation for use.

REFERENCES

1. OPPELT, E. T., Incineration of hazardous waste, a critical review, *JAPCA* 37(5), 558–586 (1987).
2. COSTNER, P. and THORNTON, J., Playing with fire: hazardous waste incineration, A Greenpeace Report, Greenpeace U.S.A., Washington, DC (1990).
3. STEVENSON, E. M., Provoking a firestorm: waste incineration, *Environ. Sci. Technol.* 25(11), 1808–1814 (1991).
4. WENDT, J. O. L., Incineration research, processes, and hearings, or the good, the bad, and the ugly, *Proceedings of the 1992 Incineration Conference*, pp. 1–5, Albuquerque, NM (May 1992).
5. GOYER, R. A., Toxic effects of metals, *Casarett and Doull's Toxicology the Basic Science of Poisons*, 4th Edn, M. O. Amdur, J. Doul and C. D. Klaassen, (Eds), Pergamon Press, New York, NY (1991).
6. VOUK, V. B. and PIVER, W. T., Metallic elements in fossil fuel combustion products: amounts and form of emissions and evaluation of carcinogenicity and mutagenicity, *Environ. Health Perspectives* 47, 201–225 (1983).
7. CLARKSON, T. W., Health effects associated with mercury contamination, *Third International Conference Municipal Waste Combustion*, Williamsburg, VA (March–April 1993).
8. CLARKSON, T. W., The role of biomarkers in reproductive and developmental toxicology, *Environ. Health Perspectives* 74, 103–107 (1987).
9. LANDRIGAN, P. J., Toxicity of lead at low dose, *Br. J. Ind. Med.* 46(9), 593–596 (1989).
10. SAROFIM, A. F. and SUK, W. A., Health effects of combustion by-products, *Environ. Health Perspectives*, in press (1992).
11. Resource conservation and recovery act, Subtitle C, Sections 3001–3013, 42 N.S.C., Sections 6921–6934 (1976) and Suppl. IV (1980) amended (1986).
12. Clean Air Act Amendments, Public Law 101–549, 104 Stat. 2399–2712, Nov. 15 (1990).
13. Federal Register, Vol. 56, No. 35, Feb. 21, 1991, U.S. EPA Office of Solid Waste, Guidance on metal and hydrogen chloride controls for hazardous waste incinerators, volume IV of the hazardous waste incineration guidance series, Hazardous waste: boilers and industrial furnaces; burning of hazardous wastes, 7134, Washington, DC (1991).
14. OSW DIRECTIVE BIF implementation document, *EPA-530/R-92-011 (NTS PB 92-154947)*, U.S. EPA, Office of Solid Waste, Washington, DC (1992).
15. FRANKEL, I., SANDERS, N. and VOGEL, G., Survey of the incinerator manufacturing industry, *Chem. Eng. Prog.* 81(3), 44–55 (1983).
16. BROOKS, G., Estimating air toxics emission from coal and oil combustion sources, *EPA-450/2-89-001 (NTIS PB89-194229)*, Environ. Prot. Agency, Research Triangle Park, NC (1989).
17. FLAGAN, R. C. and FRIEDLANDER, S. K., Particle formation in pulverized coal combustion—a review, *Recent Developments in Aerosol Science*, D. T. Shaw (Ed.), Wiley, New York, NY (1978).
18. HARDESTY, D. R. and POHL, J. H., The combustion of pulverized coals—an assessment of research needs, *National Bureau of Standards Spec. Pub. No. 561, 1407–1415* (1979).
19. Federal Register, Vol. 56, No. 28, Feb. 11, 1991, U.S. EPA Office of Air Quality Planning and Standards, Standards of performance for new stationary sources; municipal waste combustors, Research Triangle Park, NC (1991b).
20. SCOTT, D. W., Municipal Solid Waste Incineration in the United Kingdom, *2nd Int. Conf. on Municipal Waste Combustion*, 706–722, Tampa, FL (April 15–19 1991).
21. MILLOT, G., A new French plant to meet the EEC emission objectives, *Proceedings of the 1992 Incineration Conference*. pp. 759–760, Albuquerque, NM (May 1992).
22. CEFIC, Industrial waste management—a CEFIC approach to the issues, Conseil Europeen des Federations de l'Industrie Chimique (1990).
23. BIMSCHV, Bundes-Immissionsschutzgesetz Verordnung (German Federal Clean Air Act), 17 (1990).
24. HAGENMAIER, H., KRAFT, M., BRUNNER, H. and HAAG, R., Catalytic effects of flyash from waste incineration facilities on the formation and decomposition of polychlorinated dibenzo-*p*-dioxins and polychlorinated dibenzofurans, *Environ. Sci. Technol.* 21(11), 1080–1084 (1987).
25. HAGENMAIER, H., BRUNNER, H., HAAG, R. and KRAFT,

M., Copper-catalyzed dechlorination/hydrogenation of polychlorinated dibenzo-*p*-dioxins, polychlorinated dibenzofurans, and other chlorinated aromatic compounds, *Environ. Sci. Technol.* **21**(11), 1085–1088 (1987).
26. Stieglitz, L., Zwick, G., Beck, J., Roth, W. and Vogg, H., On the *de novo* synthesis of PCDD/PCDF on fly ash of municipal waste incinerators, *Chemosphere* **18**(1–6), 1219–1226 (1989).
27. Kilgroe, J. D., Combustion control of PCDD/PCDF emissions from municipal waste incinerators in North America, *10th International Meeting—Dioxin 90*, Bayreuth, F.R.G. (September 1990).
28. Kilgroe, J. D., Nelson, L. P., Schindler, P. J. and Lanier, W. S., Combustion control of organic emissions from municipal waste combustors, *Combust. Sci. Technol.* **74**, 223–244 (1990).
29. Kilgroe, J. D., Lanier, W. S. and von Alten, T. R., Montgomery county south incinerator test project: formation, emission, and control of organic pollutants, *2nd Annual Conference on Municipal Waste Combustion*, Tampa, FL (April 1991).
30. Bruce, K. R., Beach, L. O. and Gullett, B. K., The role of gas-phase Cl_2 in the formation of PCDD/PCDF during waste combustion, *Waste Manage.* **11**, 97–102 (1991).
31. Gullett, B. K., Bruce, K. R. and Beach, L. O., The effect of metal catalysts on the formation of polychlorinated dibenzo-*p*-dioxin and polychlorinated dibenzofuran precursors, *Chemosphere* **20**(10–12), 1945–1952 (1990).
32. Gullett, B. K., Bruce, K. R., Beach, L. O. and Drago, A. M., Mechanistic steps in the production of PCDD and PCDF during waste combustion, *Chemosphere* **25** (7–10), 1387–1392 (1992).
33. Queneau, P. B., May, L. D. and Cregar, D. E., Application of slag technology to recycling of solid wastes, *1991 Incineration Conference*, pp. 69–85, Knoxville, TN (May 1991).
34. Smith, J. D., Molten metal technology, *EI Digest* 8–13 (July 1991).
35. U.S. Environmental Protection Agency, Demonstration of U.S. EPA methodology for assessing health risks from indirect exposure to municipal waste combustor emissions, *EPA-600/3-91-057*, Environ. Prot. Agency, Washington, DC (September 1991).
36. California Air Pollution Control Officer's Assiciation (CAPCOA), Air toxics 'hot spots' program risk assessment guidelines, prepared by: AB2588 Risk Assessment Committee of CAPCOA, January (1992).
37. Cleverly, D. H., Rice, G. E., Durkee, S. B., Lyon, B. F. and Travis, Estimating total human exposures to toxic air pollutants emitted from the stack of municipal waste combustors, *Third International Conference Municipal Waste Combustion*, Williamsburg, VA (March–April 1993).
38. Schroeder, W. H., Dobson, M., Kane, D. M. and Johnson, N. D., Toxic trace elements associated with airborne particulate matter: a review, *JAPCA* **37**(11), 1267–1285 (1987).
39. Raask, E., *Mineral Impurities in Coal Combustion, Behavior, Problems and Remedial Measures*, Hemisphere Publishing, New York, NY (1985).
40. Gallagher, N. B., Bool, L. E., Wendt, J. O. L. and Peterson, T. W., Alkali metal partitioning in ash from pulverized coal combustion, *Combust. Sci. Technol.* **74**, 211–221 (1990).
41. Srinivasachar, S., Helble, J. J. and Boni, A. A., An experimental study of the inertial deposition of ash under coal combustion conditions, *23rd Symposium (International) on Combustion*, pp. 1305–1312, The Combustion Institute, Pittsburgh (1990).
42. Srinivasachar S., Helble, J. J. Boni, A. A. Shah, N., Huffman. G. P. and Huggins, F. E., Mineral behavior during coal combustion 2, illite transformations, *Prog. Energy Combust. Sci.*, **16**, 293–302 (1990).
43. Srinivasachar, S., Helble, J. J., Ham, D. O. and Domazetis, G., A kinetic description of vapor phase alkali transformation in combustion systems, *Prog. Energy Combust. Sci.*, **16**, 303–309 (1990).
44. Scotto, M. V., Bassham, E. A., Wendt, J. O. L., and Peterson, T. W., Quench-induced nucleation of ash constituents during combustion of pulverized coal in a laboratory furnace, *22nd Symposium (International) on Combustion*, 239–247, The Combustion Institute, Pittsburgh (1988).
45. Barta, L. E., Horvath, F., Beer, J. M. and Sarofim, A. F., Variation of mineral matter distribution in individual pulverized coal particles: application of the 'urn' model, *23rd Symposium (International) on Combustion*, pp. 1289–1296, The Combustion Institute, Pittsburgh (1990).
46. Gluskoter, H. J., *An Introduction to the Occurrence of Mineral Matter in Coal, Ash Deposits and Corrosion Due to Impurities in Combustion Gases*, R. W. Bryers (Ed.), Hemisphere Publishing, Washington, DC (1978).
47. Linak, W. P. and Peterson, T. W., Mechanisms governing the composition and size distribution of ash aerosol in a laboratory pulverized coal combustor, *21st Symposium (International) on Combustion*, pp. 399–410, The Combustion Institute, Pittsburgh (1986).
48. Holcombe, L. J., Eynon, B. P. and Switzer, P., Variability of elemental concentrations in power plant ash, *Environ. Sci. Technol.* **19**(7), 615–620 (1985).
49. Nettleton, M. A., Particulate formation in power stations boiler furnaces, *Prog. Energy Combust. Sci.* **5**, 223–243 (1979).
50. Smith, R. D., The trace element chemistry of coal during combustion and the emissions from coal fired plants, *Prog. Energy Combust. Sci.* **6**, 53–119 (1980).
51. Okazaki, K., Ohtake, K. and Nishikawa, T., Flame structure and ash particle characteristics of one-dimensional pulverized coal combustion, *1983 ASME-JSME Thermal Engineering Conf.*, Hawaii (March 1983).
52. Davison, R. L., Natusch, D. F. S., Wallace, J. R. and Evans, C. A. Jr, Trace elements in fly ash dependence of concentration on particle size, *Environ. Sci. Technol.* **8**(13), 1107–1113 (1974).
53. Kaakinen, J. W., Jorden, R. M., Lawasani, M. H. and West, R. E., Trace element behavior in coal-fired power plant, *Environ. Sci. Technol.* **9**(9), 862–869 (1975).
54. Klein, D. H., Andren, A. W., Carter, J. A., Emery, J. F., Feldman, C., Fulkerson, W., Lyon, W. S., Ogle, J. C., Talmi, Y., van Hook, R. I. and Bolton, N., Pathways of thirty-seven trace elements through coal-fired power plant, *Environ. Sci. Technol.* **9**(10), 973–979 (1975).
55. White, D. M., Edwards, L. O., Eklund, A. G., DuBose, D. A., Skinner, F. D., Richmann, D. L. and Dickerman, J. C., Correlation of coal properties with environmental control technology needs for sulfur and trace elements, *EPA-600/7-84-066 (NTIS PB84-200666)*, Environ. Prot. Agency, Research Triangle Park, NC (1984).
56. Markowski, G. R. and Filby, R., Trace element concentration as a function of particle size in fly ash in a pulverized coal utility boiler, *Environ. Sci. Technol.* **19**(9), 796–804 (1985).
57. Kauppinen, E. I. and Pakkanen, T. A., Coal combustion aerosols: a field study, *Environ. Sci. Technol.* **24**(12), 1811–1818 (1990).
58. Andren, A. W., Klein, D. H. and Talmi, Y., Selenium in coal-fired steam plant emissions, *Environ. Sci. Technol.* **9**(9), 856–858 (1975).

59. BILLINGS, C. E. and MATSON, W. R., Mercury emissions from coal combustion, *Science* **176**, 1232–1233 (1972).
60. GLADNEY, E. S., SMALL, J. A., GORDEN, G. E. and ZOLLER, W. H., Composition and size distribution of in-stack particulate material at a coal-fired power plant, *Atmos. Environ.* **10**, 1071–1077 (1976).
61. COLES, D. G., RAGAINI, R. C. and ONDOV, J. M., Behavior of natural radionuclides in western coal-fired power plants, *Environ. Sci. Technol.* **12**(4), 442–446 (1978).
62. ONDOV, J. M., RAGAINI, R. C. and BIERMANN, A. H., Elemental particle-size emissions from coal-fired power plants: use of an inertial cascade impactor, *Atmos. Environ.* **12**, 1175–1185 (1978).
63. ONDOV, J. M., RAGAINI, R. C. and BIERMANN, A. H., Elemental emissions from a coal-fired power plant. Comparison of a venturi wet scrubber system with a cold-side electrostatic precipitator, *Environ. Sci. Technol.* **13**(5), 598–607 (1979).
64. DESROSIERS, R. E., RIEHL, J. W., ULRICH, G. D. and CHIU, A. S., Submicron fly-ash formation in coal-fired boilers, *17th Symposium (International) on Combustion*, pp. 1395–1403, The Combustion Institute, Pittsburgh (1979).
65. SMITH, R. D., CAMPBELL, J. A. and NIELSON, K. K., Characterization and formation of submicron particles in coal-fired plants, *Atmos. Environ.* **13**, 607–617 (1979).
66. SMITH, R. D., CAMPBELL, J. A. and NIELSON, K. K., Volatility of fly ash and coal, *Fuel* **59**, 661–665 (1980).
67. BIERMANN, A. H. and ONDOV, J. M., Application of surface-deposition models to size-fractionated coal fly ash, *Atmos. Environ.* **14**, 289–295 (1980).
68. MARKOWSKI, G. R., ENSOR, D. S., HOOPER, R. G. and CARR, R. C., A submicron aerosol mode in flue gas from a pulverized coal utility boiler, *Environ. Sci. Technol.* **14**(11), 1400–1402 (1980).
69. FLAGAN, R. C. and TAYLOR, D. D., Laboratory studies of submicron particles from coal combustion, *18th Symposium (International) on Combustion*, pp. 1227–1237, The Combustion Institute, Pittsburgh (1981).
70. DAMLE, A. S., ENSOR, D. S. and RANADE, M. B., Coal combustion aerosol formation mechanisms: a review, *Aerosol Sci. Technol.* **1**, 119–133 (1982).
71. NEVILLE, M. and SAROFIM, A. F., The stratified composition of inorganic submicron particles produced during coal combustion, *19th Symposium (International) on Combustion*, pp. 1441–1449, The Combustion Institute, Pittsburgh (1982).
72. HAYNES, B. S., NEVILLE, M., QUANN, R. J. and SAROFIM, A. F., Factors governing the surface enrichment of fly ash in volatile trace species, *J. Colloid Interface Sci.*, **87**(1), 266–278 (1982).
73. QUANN, R. J. and SAROFIM, A. F., Vaporization of refractory oxides during pulverized coal combustion, *19th Symposium (International) on Combustion*, pp. 1429–1440, The Combustion Institute, Pittsburgh (1982).
74. QUANN, R. J., NEVILLE, M., JANGHORBANI, M., MIMS, C. A. and SAROFIM, A. F., Mineral matter and trace-element vaporization in a laboratory-pulverized coal combustion system, *Environ. Sci. Technol.* **16**(11), 776–781 (1982).
75. NEVILLE, M., MCCARTHY, J. F. and SAROFIM, A. F., Size fractionation of submicrometer coal combustion aerosol for chemical analysis, *Atmos. Environ.* **17**(12), 2599–2604 (1983).
76. SHENDRIKAR, A. D., ENSOR, D. S., COWEN, S. J., WOFFINDEN, G. J. and MCELROY, M. W., Size-dependent penetration of trace elements through a utility baghouse, *Atmos. Environ.* **17**(8), 1411–1421 (1983).
77. MCCAIN, J. D., GOOCH, J. P. and SMITH, W. B., Results of field measurements of industrial particulate sources and electrostatic precipitator performance, *JAPCA* **25**(2), 117–121 (1975).
78. SEEKER, W. R., Overview of metals behavior in combustion systems, *ASME/EPA Workship on Metals in Incineration*, Cincinnati, OH (November 1991).
79. SEEKER, W. R., Metals behavior in waste combustion systems, *International Joint Power Generation Conference*, Atlanta, GA (October 1992).
80. FUHR, H., Hazardous waste incineration at Bayer, AG, *Haz. Waste Haz. Mat.* **2**(1), 1–5 (1985).
81. BURKHOLZ, A., Measurement and separation of very fine liquid and solids particles in the chemical industry, *J. Aerosol Sci.* **22**(Suppl. 1), S513–S516 (1991).
82. THEIS, T. L. and WIRTH, J. L., Sorptive behavior of trace metals on fly ash in aqueous systems, *Environ. Sci. Technol.* **11**(12), 1096–1100 (1977).
83. WEISSMAN, S. H. CARPENTER, R. L. and NEWTON, G. J., Respirable aerosols from fluidized bed coal combustion. 3. elemental composition of fly ash, *Environ. Sci. Technol.* **17**(2), 65–71 (1983).
84. LINTON, R. W., LOH, A. and NATUSCH, D. F. S., Surface predominance of trace elements in airborne particles, *Science* **191**, 852–854 (1976).
85. LINAK, W. P. and Peterson, T. W., Effect of coal type and residence time on the submicron aerosol distribution from pulverized coal combustion, *Aerosol Sci. Technol.* **3**, 77–96 (1984).
86. BULEWICZ, E. M., EVANS, D. G. and PADLEY, Effect of metallic additives on soot formation processes in flames, *15th Symposium (International) on Combustion*, pp. 1461–1470, The Combustion Institute, Pittsburgh (1974).
87. HAYNES, B. S., JANDER, H. and WAGNER, H. G., The effect of metal additives on the formation of soot in premixed flames, *17th Symposium (International) on Combustion*, pp. 1365–1381, The Combustion Institute, Pittsburgh (1978).
88. FELDMAN, N., Control of residual fuel oil particulate emissions by additives, *19th Symposium (International) on Combustion*, pp. 1387–1393, The Combustion Institute, Pittsburgh (1982).
89. CHUNG, S. L. and LAI, N. L., Suppression of soot by metal additives during the combustion of polystyrene, *J. Air Waste Manag. Assoc.*, **42**(8), 1082–1088 (1992).
90. PIPER, B. and NAZIMOWITZ, W., High viscosity oil evaluation, 59th street station—unit 110, Vol. 1, KVB report to Consolidated Edison Co., 21640-1 (March 1985).
91. WALSH, P. M., WEI, G. and XIE, J., Metal oxide and coke particulates formed during combustion of residual fuel oil, *10th Annual Meeting American Assoc. for Aerosol Research*, 7P.36, Traverse City, MI (October 1991).
92. BUERKI, P. R., GAELLI, B. C. and NYFFELER, U. P., Size-resolved trace metal characterization of aerosols emitted by four important source types in Switzerland, *Atmos. Environ.* **23**(8), 1659–1668 (1989).
93. BACCI, P., DEL MONTE, M., LONGHETTO, A., PIANO, A., PRODI, F., REDAELLI, P., SABBIONI, C. and VENTURA, A., Characterization of the particulate emission by a large oil fuel fired power plant, *J. Aerosol Sci.* **14**(4), 557–572 (1983).
94. MUMFORD, J. L., HATCH, G. E., HALL, R. E., JACKSON, M. A., MERRILL, R. G. and LEWTAS, J., Toxicity of particles emitted from combustion of waste crankcase oil: *in vitro* and *in vivo* studies, *Fund. Appl. Toxicol.* **7**, 49–57 (1986).
95. TRICHON, M. and FELDMAN, J., Chemical kinetic considerations of trace toxic metals in incinerators, *1989 Incineration Conference*, 9.1.1–9.1.18, Knoxville, TN (May 1989).
96. TRICHON, M. and FELDMAN, J., Problems associated with the detection and measurement of arsenic in incin-

erator emissions, *1991 Incineration Conference*, pp. 571–579, Knoxville, TN (May 1991).
97. Oberacker, D. A., Overview of Superfund waste characteristics, relative to incineration, *ASME/EPA Workshop on Metals in Incineration*, Cincinnati, OH (November 1991).
98. Waterland, L. R., King, C., Vocque, R. H., Richards, M. K. and Wall, H. O., Pilot-scale incinerability evaluation of arsenic- and lead-contaminated soils from two superfund sites, *1991 Incineration Conference*, pp. 335–344, Knoxville, TN (May 1991).
99. Seeker, W. R., Waste combustion, *23rd Symposium (International) on Combustion*, pp. 867–885, The Combustion Institute, Pittsburgh (1990).
100. Linak, W. P., Kilgroe, J. D., McSorley, J. A., Wendt, J. O. L. and Dunn, J. E., On the occurrence of transient puffs in a rotary kiln incinerator simulator: I. prototype solid plastic wastes, *J. Air Pollut. Control Assoc.* 37(1), 54–65 (1987).
101. Linak, W. P., McSorley, J. A., Wendt, J. O. L. and Dunn, J. E., On the occurrence of transient puffs in a rotary kiln incinerator simulator: II. contained liquid wastes on sorbent, *J. Air Pollut. Control Assoc.* 37(8), 934–942 (1987).
102. Lighty, J. S., Eddings, E. G., Lingren, E. R., Xaio-Xue, D., Pershing, D. W., Winter, R. M. and McClennen, W. H., Rate limiting processes in the rotary-kiln incineration of contaminated soils, *Combust. Sci. Technol.* 74, 31–49 (1990).
103. Litt, R. D. and Tewksbury, T. L., Trace metal retention when firing hazardous waste in a fluidized-bed incinerator, *EPA-600/2-84-198 (NTIS PB85-138618)*, Environ. Prot. Agency, Research Triangle Park, NC (1984).
104. Wallace, D. D., Trenholm, A. R. and Lane, D. D., Assessment of metal emissions from hazardous waste incinerators, *78th Annual Meeting of the Air Pollution Control Association*, Detroit, MI (June 1985).
105. Mournighan, R. E., Lee, J. W., Ross, R. W. and Vocque, R. H., Distribution of volatile and trace elements in emissions and residuals from pilot-scale liquid injection incineration, *1987, AFRC International Symposium on Incineration of Hazardous, Municipal, and Other Wastes*, Palm Springs, CA (November 1987).
106. Barton, R. G., Maly, P. M., Clark, W. D. and Seeker, W. R., Prediction of the fate of toxic metals in waste incinerators, *1988 National ASME Waste Processing Conference* (1988).
107. Barton, R. G., Clark, W. D. and Seeker, W. R., Fate of metals in waste combustion systems, *Combust. Sci. Technol.* 74, 327–342 (1990).
108. Lee, C. C., A model analysis of metal partitioning, *JAPCA* 38(7), 941–945 (1988).
109. Fournier, D. J. and Waterland, L. R., The fate of trace metals in a rotary kiln incinerator with a single-stage ionizing wet scrubber, *EPA-600/D-90-059 (NTIS PB90-246174)*, Environ. Prot. Agency, Cincinnati, OH (1989).
110. Fournier, D. J., Whitworth, W. E., Lee, J. W. and Waterland, L. R., The fate of trace metals in a rotary kiln incinerator with a venturi/packed column scrubber Vol. I technical results, *EPA-600/2-90-043a (NTIS PB90-263864)*, Environ. Prot. Agency, Cincinnati, OH (1990).
111. Fournier, D. J., Waterland, L. R., Lee, J. W. and Carroll, G. J., The behavior of trace metals in rotary kiln incineration: results of incineration research facility studies, *Proceedings of the 17th Annual RREL Hazardous Waste Research Symposium, EPA-600/9-91-002 (NTIS PB91-233627)*, pp. 172–189, Environ. Prot. Agency, Cincinnati, OH (April 1991).
112. Carroll, G. J., Thurnau, R. C. Mournighan, R. E., Waterland, L. R., Lee, J. W. and Fournier, D. J., The partitioning of metals in rotary kiln incineration, *EPA-600/D-89-208 (NTIS PB90-132812)*, Environ. Prot. Agency, Cincinnati, OH (1991).
113. Thurnau, R. C. and Fournier, D., The behavior of arsenic in a rotary kiln incinerator, *J. Air Waste Manage. Assoc.* 42(2), 179–184 (1992).
114. Burton, B. K., Status and directions of the U.S. municipal waste combustion industry, *Third International Conference Municipal Waste Combustion*, Williamsburg, VA (March–April 1993).
115. Berenyi, E., A decade of municipal waste combustion in the United States: prospects and problems, *Third International Conference Municipal Waste Combustion*, Williamsburg, VA (March–April 1993).
116. Lisk, D. J., Environmental implications of incineration of municipal solid waste ash disposal, *Sci. Total Environ.* 74, 39–66 (1988).
117. Environment Canada, National incinerator testing and evaluation program: environmental characterization of mass burning incinerator technology at Quebec City, *Environ. Can. Rep. EPS 3/UP/5*, Ottawa, Ontario, June (1988).
118. Kiser, J. V. L., Municipal waste combustion in north America: 1992 update, *Waste Age* 23(11), 1–6 (1992).
119. Kiser, J. V. L., Municipal waste combustion in north America: 1992 update, reprinted in: *Status of Municipal Waste Combustion in the United States: 1992 Update*, Integrated Waste Services Association, Washington, DC (1992).
120. National Solid Wastes Management Association, The 1992 municipal waste combustion guide, *Waste Age* 23(11), 17–35 (1992).
121. National Solid Wastes Management Association, *The 1992 Municipal Waste Combustion Guide*, reprinted in *Status of Municipal Waste Combustion in the United States: 1992 Update*, Integrated Waste Services Association, Washington, DC (1992b).
122. Greenberg, R. R., Zoller, W. H. and Gordon, G. E., Composition and size distributions of particles released in refuse incineration, *Environ. Sci. Technol.* 12(5), 566–573 (1978).
123. Law, S. L. and Gordon, G. E., Sources of metals in municipal incinerator emissions, *Environ. Sci. Technol.* 13(4), 432–438 (1979).
124. Korzun, E. A. and Heck, H. H., Sources and fates of lead and cadmium in municipal solid waste, *J. Air Waste Manag. Assoc.* 40(9), 1220–1226 (1990).
125. Vogg, H., Braun, H., Metzger, M. and Schneider, J., The specific role of cadmium and mercury in municipal solid waste incineration, *Waste Manag. Res.* 4, 65–74 (1986).
126. Hall, B., Lindqvist, O. and Ljungstrom, E., Mercury chemistry in simulated flue gases related to waste incineration conditions, *Environ. Sci. Technol.* 24(1), 108–111 (1990).
127. Scheil, G., Klamm, S., Whitacre, M., Surman, J. and Kelly, W., Municipal waste combustion multipollutant study emission test report Maine Energy Recovery Company refuse derived fuel facility Biddeford, Maine, Vol. 1: summary of results, *EPA-600/8-89-064a (NTIS PB90-228834)*, Environ. Prot. Agency, Research Triangle Park, NC (1989).
128. Brna, T. G., Toxic metal emissions from MWCs and their control, *2nd Annual Conference on Municipal Waste Combustion*, Tampa, FL (April 1991).
129. Brna, T. G. and Kilgroe, J. D., The impact of particulate emissions control on the control of other MWC air emissions, *J. Air Waste Manage. Assoc.* 40(9), 1324–1330 (1990).
130. Otani, Y., Kanaoka, C., Usui, C., Matsui, S. and Emi, H., Adsorption of mercury vapor on particles, *Environ. Sci. Technol.* 20(7), 735–738 (1986).
131. Otani, Y., Emi, H., Kanaoka, C., Uchijima, I. and

NISHINO, H., Removal of mercury vapor from air with sulfur-impregnated adsorbents, *Environ. Sci. Technol.* 22(6), 708–711 (1988).
132. NORTON, G. A., DEKALB, E. L. and MALABY, K. L., Elemental composition of suspended particulate matter from the combustion of coal and coal/refuse mixtures, *Environ. Sci. Technol.* 20(6), 604–609 (1986).
133. NORTON, G. A., MALABY, K. L. and DEKALB, E. L., Chemical characterization of ash produced during combustion of refuse-derived fuel with coal, *Environ. Sci. Technol.* 22(11), 1279–1283 (1988).
134. ALLEN, R. J., BRENNIMAN, G. R. and DARLING, C., Air pollution emissions from the incineration of hospital waste, *JAPCA* 36(7), 829–831 (1986).
135. KAUPPINEN, E. I. and PAKKANEN, T. A., Mass and trace element size distributions of aerosols emitted by a hospital refuse incinerator, *Atmos. Environ.* 24A(2), 423–429 (1990).
136. CARTLEDGE, F. K., BUTLER, L. G., CHALASANI, D., EATON, H. C., FREY, F. P., HERRERA, E., TITTLEBAUM, M. E. and YANG, S. L., Immobilization mechanisms in solidification/stabilization of Cd and Pb salts using portland cement fixing agents, *Environ. Sci. Technol.* 24(6), 867–873 (1990).
137. GOSSMAN, D., The fate of trace metals in wet process cement kilns, *AWMA Specialty Conference on Waste Combustion in Boilers and Industrial Furnaces*, pp. 70–93, Kansas City, MO (April 1990).
138. HARRISON, R. M. and WILLIAMS, C. R., Physico-chemical characterization of atmospheric trace metal emissions from a primary zinc–lead smelter, *Sci. Total Environ.* 31, 129–140 (1983).
139. SHEN, T. T., Air pollution from sewage sludge incineration, *J. Environ. Eng. Div.* 61–74 (February 1979).
140. BENNETT, R. L. and KNAPP, K. T., Characterization of particulate emissions from municipal wastewater sludge incinerators, *Environ. Sci. Technol.* 16(12), 831–836 (1982).
141. DEWLING, R. T., MANGANELLI, R. M. and BAER, G. T., Fate and behavior of selected heavy metals in incinerated sludge, *J. WPCF* 52(10), 2553–2557 (1980).
142. KISTLER, R. C., WIDMER, F. and BRUNNER, P. H., Behavior of chromium, nickel, copper, zinc, cadmium, mercury, and lead during the pyrolysis of sewage sludge, *Environ. Sci. Technol.* 21(7), 704–708 (1987).
143. EDDINGS, E. G. and LIGHTY, J. S., Fundamental studies of metal behavior during solids incineration, *Combust. Sci. Technol.* 85, 375–485 (1992).
144. BHATIA, R. and SIRIGNANO, W. A., Vaporization and combustion of metal slurry droplets, *29th Aerospace Sciences Meeting, AIAA-91-0282*, Reno, NV (January 1991).
145. MULHOLLAND, J. A. and SAROFIM, A. F., Mechanisms of inorganic particle formation during suspension heating of simulated aqueous wastes, *Environ. Sci. Technol.* 25(2), 268–274 (1991).
146. EBBINGHAUS, B. B., Analysis of chromium volatility in the DWTF incinerator and in the molten salt processor, *Proceedings of the 1992 Incineration Conference*, pp. 599–604, Albuquerque, NM (May 1992).
147. GORDON, S. and MCBRIDE, B. J., Computer program for calculation of complex chemical equilibrium compositions, rocket performance, incident and reflected shocks, and Chapman–Jouguet detonations, *NASA SP-273*, Interim Revision (March 1986).
148. SCOTTO, M. A., PETERSON, T. W. and WENDT, J. O. L., Hazardous waste incineration: the *in situ* capture of lead by sorbents in a laboratory down-flow combustor, *24th Symposium (International) on Combustion*, pp. 1109–1118, The Combustion Institute, Pittsburgh (1992).
149. MULHOLLAND, J. A., SAROFIM, A. F. and YUE, G., The formation of inorganic particles during suspension heating of simulated wastes, *Environ. Prog.* 10(2), 83–88 (1991).
150. SCOTTO, M. V., PETERSON, T. W. and WENDT, J. O. L., Suppression of Pb aerosol from combustion processes by sorbent injection, *Second International Congress on Toxic Combustion By-Products: Formation and Control*, Salt Lake City, UT (March 1991).
151. NEVILLE, M. and SAROFIM, A. F., The fate of sodium during pulverized coal combustion, *Fuel* 64, 384–490 (1985).
152. MIMS, C. A., NEVILLE, M., QUANN, R. J., HOUSE, K. and SAROFIM, A. F., Laboratory studies of mineral matter vaporization during coal combustion, *AIChE Symposium Series* 76(201), 188–194 (1980).
153. WIBBERLY, L. J. and WALL, T. F., Alkali-ash reactions and deposit formation in pulverized-coal-fired boilers: experimental aspects of sodium silicate formation and the formation of deposits, *Fuel* 61, 93–99 (1982).
154. LINDER, E. R. and WALL, T. F., Sodium ash reactions during combustion of pulverized coal, *23rd Symposium (International) on Combustion*, pp. 1313–1321, The Combustion Institute, Pittsburgh (1990).
155. GALLAGHER, N., PETERSON, T. W. and WENDT, J. O. L., Alkali/silicate interactions during pulverized coal combustion, *201st ACS Natl Meeting Preprints* 36(1), 181–190 (1991).
156. GALLAGHER, N. B., BOOL, L. E., WENDT, J. O. L. and PETERSON, T. W., Alkali/silicate interactions during pulverized coal combustion, *ACS Div. of Fuel Chem.*, Atlanta, GA (April 1991).
157. HELBLE, J. J., SRINIVASACHAR, S. and BONI, A. A., Factors influencing the transformation of minerals during pulverized coal combustion, *Prog. Energy Combust. Sci.* 16, 267–279 (1990).
158. GALLAGHER, N. B., Alkali metal partitioning in a pulverized coal combustion environment, Ph.D. Dissertation, University of Arizona, Tucson, AZ (1992).
159. SENIOR, C. L. and FLAGAN, R. C., Synthetic chars for the study of ash vaporization, *20th Symposium (International) on Combustion*, pp. 921–929, The Combustion Institute, Pittsburgh (1984).
160. PUNJAK, W. A., UBEROI, M. and SHADMAN, F., High-temperature adsorption of alkali vapors on solid sorbents, *AIChE J.* 35(7), 1186–1194 (1989).
161. LIGHTY, J. S. and EDDINGS, E. G., A study of metal contaminant behavior in a pilot-scale rotary kiln, *24th Symposium (International) on Combustion*, Sydney, Australia (July 1992).
162. FRIEDLANDER, S. K., *Smoke Dust and Haze—Fundamentals of Aerosol Behavior*, Wiley, New York, NY (1977).
163. SMOULOCHOWSKI, M., Versuch einer mathematischen Theorie der Koagulationskinetic kolloider Losungen,' *Z. Physik Chem.* 92, 129–168 (1917).
164. FUCHS, N. A., *The Mechanics of Aerosols*, C. N. Davies (Ed.), Pergamon Press, Oxford (1964).
165. SWIFT, D. L. and FRIEDLANDER, S. K., The coagulation of hydrosols by Brownian motion and laminar shear flow. *J. Colloid Interface Sci.* 19, 621–647 (1964).
166. FRIEDLANDER, S. K. and WANG, C. S., The self-preserving particle size distribution for coagulation by Brownian motion, *J. Colloid Interface Sci.* 22, 126–132 (1966).
167. KOCH, W. and FRIEDLANDER, S. K., The effect of particle coalescence on the surface area of a coagulating aerosol, *J. Colloid Interface Sci.* 140(2), 419–427 (1990).
168. MATSOUKAS, T. and FRIEDLANDER, S. K., Dynamics of aerosol agglomerate formation, *J. Colloid Interface Sci.* 146(2), 495–506 (1991).

169. Levich, V. G., *Physiochemical Hydrodynamics* (English translation), Prentice Hall, Englewood Cliffs, NJ (1962).
170. Gelbard, F. and Seinfeld, J. H., Simulation of multicomponent aerosol dynamics, *J. Colloid Interface Sci.* **78**(2), 485–501 (1980).
171. Gelbard, F. and Seinfeld, J. H., Numerical solution of the dynamic equation for particulate systems, *J. Comp. Phys.* **28**(3), 357–375 (1978).
172. Gelbard, F. and Seinfeld, J. H., Coagulation and growth of a multicomponent aerosol. *J. Colloid Interface Sci.* **63**(3), 472–479 (1978).
173. Gelbard, F. and Seinfeld, J. H., The general dynamic equation for aerosols–theory and application to aerosol formation and growth, *J. Colloid Interface Sci.* **68**(2), 363–382 (1979).
174. Gelbard, F., Tambour, Y. and Seinfeld, J. H., Sectional representations for simulating aerosol dynamics, *J. Colloid Interface Sci.*, **76**(2), 541–556 (1980).
175. Friedlander, S. K., Koch, W. and Main, H. H., Scavenging of a coagulating fine aersol by a coarse particle mode, *J. Aerosol Sci.* **22**(1), 1–8 (1991).
176. Sethi, V. and Biswas, P., Modeling of particle formation and dynamics in a flame incinerator, *J. Air Waste Manage. Assoc.* **40**(1), 42–46 (1990).
177. Sethi, V. and Biswas, P., Fundamental studies on particulate emissions from hazardous waste incinerators, In Proceedings: *16th Annual EPA Research Symposium Remedial Action, Treatment, and Disposal of Hazardous Waste, EPA-600/9-90-037* (*NTIS PB91-148379*), Cincinnati, OH (April 1990b).
178. Lin, W. Y., Sethi, V. and Biswas, P., Multicomponent aerosol dynamics of the Pb–O_2 system in a bench scale flame incinerator, *Aerosol Sci. Technol.* **17**, 119–133 (1992).
179. Biswas, P., Lin, W. Y. and Wu, C. Y., Fate of metallic constituents during incineration, *Proceedings of the 1992 Incineration Conference*, pp. 595–598, Albuquerque, NM (May 1992).
180. McNallan, M. J., Yurek, G. J. and Elliott, J. F., The formation of inorganic particulates by homogeneous nucleation in gases produced by the combustion of coal, *Combust. Flame* **42**, 45–60 (1981).
181. Fuchs, N. A. and Sutugin, A. G. *Topics in Current Aerosol Research*, G. M. Hidy and J. R. Brock (Eds), Pergamon Press, New York, NY (1971).
182 Petersen, E. E., *Chemical Reaction Analysis*, Prentice Hall, Englewood Cliffs, NJ (1965).
183. McMurry, P. H. and Friedlander, S. K., New particle formation in the presence of an aerosol, *Atmos. Environ.* **13**, 1635–1651 (1979).
184. Frenkel, J., *Kinetic Theory of Liquids*, Dover Press, New York, NY (1955).
185. Senior, C. L. and Flagan, R. C., Ash vaporization and condensation during combustion of a suspended coal particle, *Aerosol Sci. Technol.* **1**, 371–383 (1982).
186. Helble, J., Neville, M. and Sarofim, A. F., Aggregate formation from vaporized ash during pulverized coal combustion, *21st Symposium (International) on Combustion*, pp. 411–417, The Combustion Institute, Pittsburgh (1986).
187. Taylor, D. D. and Flagan, R. C., The influence of combustor operation on fine particles from coal combustion, *Aerosol Sci. Technol.* **1**, 103–117 (1982).
188. Uberoi, M. and Shadman, F., Sorbents for the removal of lead compounds from hot flue gases, *AIChE J.* **36**(2), 307–309 (1990).
189. Uberoi, M. and Shadman, F., High-temperature removal of cadmium compounds using sorbents, *Environ. Sci. Technol.* **25**(7), 1285–1289 (1991).
190. Uberoi, M., High Temperature removal of metal vapors by solid sorbents, Ph.D. Dissertation, University of Arizona, Tucson, AZ (1990).
191. Uberoi, M., Punjak, W. A. and Shadman, F., The kinetics and mechanism of alkali removal from flue gases by solid sorbents, *Prog. Energy Combust. Sci.* **16**, 205–211 (1990).
192. Ho, T. C., Chen, C., Hopper, J. R. and Oberacker, D. A., Fluidized bed technology for metal emission control, *1991 AIChE National Meeting*, Pittsburgh, PA (August 1991).
193. Ho, T. C., Tan, L., Chen, C. and Hopper, J. R., Characteristics of metal capture during fluidized bed incineration, *AIChE Symposium Series* **87**(281), 118–126 (1991).
194. Ho, T. C., Chen, C., Hopper, J. R. and Oberacker, D. A., Metal capture during fluidized bed incineration of wastes contaminated with lead chloride, *Combust. Sci. Technol.* **85**, 101–116 (1992).